

Quantum Kinetic and Inertial Alfven Waves: Linear and Nonlinear Analysis



By

NAUMAN SADIQ

44-FBAS/PHDPHY/S15

Supervisor:

Dr. MUSHTAQ AHMAD

**DEPARTMENT OF PHYSICS, FBAS,
INTERNATIONAL ISLAMIC UNIVERSITY,
ISLAMABAD**

2020

Quantum Kinetic and Inertial Alfvén Waves: Linear and Nonlinear Analysis

By

NAUMAN SADIQ

44-FBAS/PHDPHY/S15

A thesis is submitted to

Department of Physics

For the award of the degree of

PHD Physics

Signature..........

(Chairman, Department of Physics)

Signature..........

(Dean FBAS, IIU Islamabad)

**DEPARTMENT OF PHYSICS, FBAS,
INTERNATIONAL ISLAMIC UNIVERSITY**

ISLAMABAD

2020

PHD
530 12
NAD

Q Accession No 7423125

Quantum Theory
Physics

Final Approval

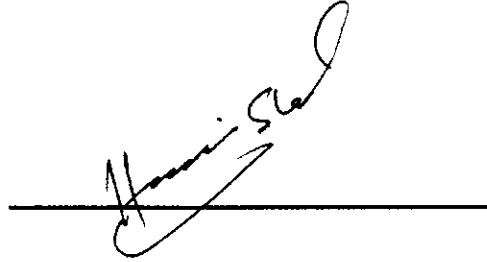
It is certified that the work presented in this thesis having title “**Quantum Kinetic and Inertial Alfvén Waves: Linear and Nonlinear Analysis**” by NAUMAN SADIQ (Reg. No. 44-FBAS/PHDPHY/S15) fulfill the requirement for the award of degree of Ph.D Physics from Department of Physics, International Islamic University, Islamabad, Pakistan.

Viva Voice Committee

Chairman

Dr. Wiqar Hussain Shah

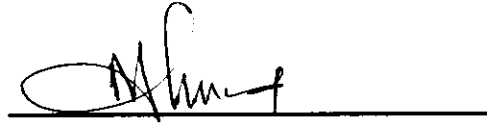
Associate Professor



Supervisor

Dr. Mushtaq Ahmad

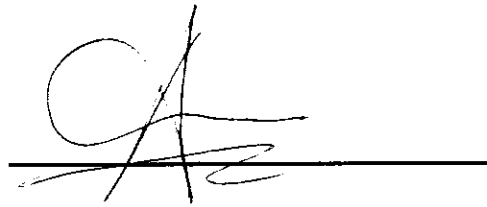
Professor



External Examiner

Dr. Arshad Majid Mirza


Professor



External Examiner

Dr. Aman ur Rehman

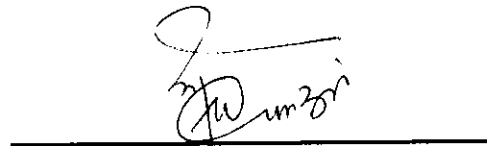
Professor



Internal Examiner

Dr. Zafar Wazir

Assistant Professor



Dedicated to

My Mother, Wife, and Daughters (Amarha and Baqish)

For Their

Love, Support and Prayers

DECLARATION

I hereby declare that the work presented in this thesis is produced by me during the scheduled course of time. My name in all the publications is written as N. Sadiq. It is further declared that this thesis neither as a whole nor as a part thereof has been copied out from any source except referred by me whenever due. No portion of the work presented in this thesis has been submitted in support of any other degree or qualification of this or any other university or institute of learning. If any violation of HEC rules on research has occurred in this thesis, I shall be liable to punishable action under the plagiarism rules of Higher Education Commission (HEC) Pakistan.

NAUMAN SADIQ

44-FBAS/PHDPHY/S15

ACKNOWLEDGEMENTS

All Praises to Almighty Allah, the most benevolent and merciful and the Creator of the universe, who enabled me to complete this research work successfully. And Darood-o- Salam to Holy Prophet (Peace Be Upon Him) who is forever a torch of guidance and knowledge for the whole humanity.

I would like to express my sincere and hearty appreciation to my supervisor Dr. Mushtaq Ahmad for his constant encouragement, invaluable guidance, mentorship and helpful suggestions during this research work. I deeply appreciate his energy, enthusiasm, and ability to see and formulate new and exciting physical problems. He always displayed tolerance and patience as I have transitioned from a struggling student to a plasma physicist. I also would like to express gratitude for his moral support during crucial periods of my research work.

I acknowledge the co-operation and encouragement extended to me by the Head, faculty, and staff of the physics department IIUI for being very supportive and cooperative throughout my research work. I also pay thanks to my Ph.D. colleagues Muhammad Farooq, Qasim Jan, Safdar Ali, Saeed Anwar, Sadiq Usman, Shah Fahad, Akhtar Iqbal as well as MS fellows for being very helpful in all my research work.

Finally, my deepest gratitude goes to my loving mother, my caring wife and my daughters who suffered but always prayed for my success and supported me. Without their care, support, comfort, and comradeship, I would not enjoy the successes I have achieved to this day. I would also like to pay compliments to my brothers, sisters and friends who remained with me throughout the whole journey.

May Allah bless all these people (Ameen).

Nauman Sadiq

Abstract

In this thesis, we have studied linear and nonlinear propagation characteristics of kinetic and inertial Alfvén waves in homogenous, non-relativistic, collisionless low- β electron-ion magnetized quantum plasmas by considering arbitrary temperature degeneracy, spin magnetization, and exchange-correlation effects. Using the quantum magnetohydrodynamic fluid model, both the Sagdeev potential approach and Korteweg de Vries equation have derived to get nonlinear solution of the set of partial differential equations in the form of solitary pulses in laboratory, space, and astrophysical plasmas settings.

Linear and nonlinear kinetic Alfvén waves (KAWs) with an effect of arbitrary temperature degeneracy have been investigated in low- β quantum plasma. The linear analysis of KAWs shows an increase (decrease) in frequency with the increase of parameter $\zeta(\delta)$ for nearly non-degenerate (nearly degenerate) plasmas limit. On the other hand, nonlinear analysis reveals that the amplitude of the Sagdeev potential curves and soliton structures remains the same but the potential depth and width of soliton structure change for nearly non-degenerate and nearly degenerate limiting cases. It is further observed that only density hump structures are formed in the sub-Alfvénic region.

The effects of spin magnetization on linear and nonlinear KAWs have also been studied in low- β dense quantum plasma. The numerical analysis illustrates that the dynamics of linear and nonlinear structures are appreciably modified due to the change in spin magnetization effects. Moreover, it is found that only density hump structures are formed in the sub-Alfvénic region.

Moreover, we have investigated solitary inertial Alfvén waves (IAWs) in an intermediate β quantum plasma, considering electron temperature degeneracy correction. It is found that in the presence of electron inertia and thermal pressure, the inertial Alfvén solitary waves accompanied by both hump and dip solitons.

Additionally, the effect of electron exchange-correlation and spin magnetization on solitary IAWs in quantum plasma have also been discussed. It is found that inertial Alfvén solitons with a density dip exist. The spin magnetization effects are more dominant in a quantum plasma model than exchange-correlation effects.

List of Publications

This thesis is based on the following four publications:

1. **Nauman Sadiq**, Mushtaq Ahmad, M. Farooq, and Qasim Jan, "*Linear and nonlinear analysis of kinetic Alfvén waves in quantum magneto-plasmas with arbitrary temperature degeneracy*", *Physics of Plasmas* **25** 063510 (2018)-AIP Journal.
2. **Nauman Sadiq** and A. Mushtaq, "*Inertial Alfvén solitons in quantum plasma with correction of temperature degeneracy*" *Physics of Plasmas* **25** 124501 (2018)-AIP Journal.
3. **Nauman Sadiq** and Mushtaq Ahmad, "*Kinetic Alfvén waves in dense quantum plasmas with effect of spin magnetization*", *Plasma Research Express* **1** 025007 (2019)-IOP Journal.
4. **Nauman Sadiq** and Mushtaq Ahmad, "*Quantum inertial Alfvén solitary waves: The effects of exchange-correlation and spin magnetization*", *Journal of Waves in Random and Complex Media*, (2020)-Taylor & Francis Online. DOI: 10.1080/17455030.2020.1718243.

Contents

1	Introduction	5
1.1	Plasma Physics	5
1.2	Quantum Plasmas	6
1.3	Quantum Magnetohydrodynamics	7
1.4	Fermi-Dirac Statistics and Temperature Degeneracy	8
1.5	Kinetic and Inertial Alfvén Waves	11
1.6	Theory of Solitons	13
1.6.1	Korteweg-de Vries Equation	13
1.6.2	Sagdeev's Pseudopotential Method	14
1.7	Layout of the Thesis	15
2	Kinetic Alfvén waves in quantum plasmas with arbitrary temperature degeneracy	18
2.1	Introduction	18
2.2	Model Equations	20
2.2.1	Linear Wave Analysis	25
2.2.2	Nonlinear Wave Analysis	26
2.3	Numerical Analysis and Discussion	29
2.4	Conclusion	34
3	The effect of spin magnetization on Kinetic Alfvén waves in dense plasmas	35
3.1	Introduction	35
3.2	Formulation	38

3.3	Numerical Analysis and Discussion	42
3.4	Conclusion	46
4	Inertial Alfvén waves in quantum plasma with correction of temperature degeneracy	47
4.1	Introduction	47
4.2	Basic Equations	50
4.3	Numerical Analysis and Discussion	55
4.4	Conclusion	57
5	The effect of exchange-correlation and spin magnetization on inertial Alfvén waves in dense plasma	59
5.1	Introduction	59
5.2	Basic Equations	61
5.2.1	Derivation of Sagdeev's Potential	65
5.2.2	Derivation of KdV Equation	66
5.3	Numerical Analysis and Discussion	69
5.4	Summary	73
	Bibliography	75

List of Figures

1.1	$f(\varepsilon)$ at $T_e = 0$	9
1.2	$f(\varepsilon)$ at different temperatures.	10
2.1	Plot of (normalized) frequency ω with respect to (normalized) wavenumber k_x from Eq.(2.28) (nearly non-degenerate plasma) for different values of ζ such that $\zeta = 10^{-4}$ (blue, bold) with $T_e = 2.0 \times 10^4$ ($^{\circ}K$), $n_0 = 1.37 \times 10^{24}$ (m^{-3}) , $\zeta = 10^{-3}$ (blue, dashed) with $T_e = 9.2 \times 10^4$ ($^{\circ}K$), $n_0 = 1.37 \times 10^{26}$ (m^{-3}) and $\zeta = 10^{-2}$ (red,dashed) with $T_e = 4.3 \times 10^5$ ($^{\circ}K$), $n_0 = 1.35 \times 10^{28}$ (m^{-3}). Other parameters are $B_0 = 1$ Tesla, $g = 0.1$, $\frac{k_z}{k_0} = 0.1$ and $k_0 = 12500$	30
2.2	The (normalized) frequency ω is plotted against (normalized) wavenumber k_x from Eq.(2.29) (nearly degenerate plasma) for different values of δ such that $\delta = 10^{-4}$ (blue,bold) with $T_F = 4.78 \times 10^7$ ($^{\circ}K$), $T_e = 4780$ ($^{\circ}K$), $n_0 = 1.21 \times 10^{33}$ (m^{-3}) , $\delta = 10^{-3.7}$ (blue.dashed) with $T_F = 4.78 \times 10^7$ ($^{\circ}K$), $T_e = 9538.13$ ($^{\circ}K$), $n_0 = 1.21 \times 10^{33}m^{-3}$ and $\delta = 10^{-3.4}$ (red,dashed) with $T_F = 4.78 \times 10^7$ ($^{\circ}K$), $T_e = 19031.1$ ($^{\circ}K$), $n_0 = 1.21 \times 10^{33}$ (m^{-3}). Other parameters are $B_0 = 5.4 \times 10^3$ Tesla, $g = 0.1$, $\frac{k_z}{k_0} = 0.1$ and $k_0 = 12500$	31
2.3	Plots of Sagdeev potential U from Eq.(2.56) against number density n for different values of ζ such that $\zeta = 0.1$ (blue, bold) with $T_e = 1.9 \times 10^6$ ($^{\circ}K$), $n_0 = 1.21 \times 10^{30}$ (m^{-3}), $\zeta = 0.45$ (blue, dashed) with $T_e = 4.3 \times 10^6$ ($^{\circ}K$), $n_0 = 1.72 \times 10^{31}$ (m^{-3}) and $\zeta = 0.8$ (red,dashed) with $T_e = 5.5 \times 10^6$ ($^{\circ}K$), $n_0 = 4.08 \times 10^{31}$ (m^{-3}) for nearly non-degenerate plasma limit, while keeping $K_z = \sqrt{1.5}$ and $K_x = \sqrt{1 - K_z^2}$, with $g = 0.1$	32

2.4	Variation of soliton structure of δn versus η from Eq.(2.57) for nearly non-degenerate plasma. All parameters are the same as in Fig. 2.3.	32
2.5	Sagdeev potential U is plotted against number density n from Eq.(2.58) for nearly degenerate plasma with same values of δ as in Figure 2.2, while keeping $K_z = \sqrt{1.5}$ and $K_x = \sqrt{1 - K_z^2}$, with $g = 0.1$	33
2.6	The soliton profile of δn versus η from Eq.(2.59) for nearly degenerate plasma. All parameters are the same as in Figure 2.5.	34
3.1	Plot of (normalized) frequency ω with respect to (normalized) wavenumber k_x of Eq.(3.13) for different values of plasma number density such that (i) $n_0 \approx 6.38 \times 10^{33} (m^{-3})$ (Bold, Black) with $g_Q = 0.0345$, $T_F \approx 1.4 \times 10^8(^{\circ}K)$, $H \approx 0.00049$, $\varepsilon_0 \approx 0.00046$. (ii) $n_0 \approx 1.78 \times 10^{34} (m^{-3})$ (Dashed, Red) with $g_Q = 0.0245$, $T_F \approx 2.86 \times 10^8(^{\circ}K)$, $H \approx 0.00059$, $\varepsilon_0 \approx 0.00023$. (iii) $n_0 \approx 8.59 \times 10^{34} (m^{-3})$ (DotDashed, Blue) with $g_Q = 0.0145$, $T_F \approx 8.18 \times 10^8(^{\circ}K)$, $H \approx 0.00076$, $\varepsilon_0 \approx 0.000081$. Other parameters are $l_z = 0.99$, $B_0 = 10^5(Tesla)$	43
3.2	Plot of (normalized) frequency ω with respect to (normalized) wavenumber k_x of Eq.(3.13) for different values of magnetic field strength (i.e. spin magnetization energy) such that (i) $B_0 = 2.0 \times 10^8(Tesla)$ (Bold, Black) with $\varepsilon_0 \approx 1.54$. (ii) $B_0 = 3.0 \times 10^8(Tesla)$ (Dashed, Red) with $\varepsilon_0 \approx 2.30$. (iii) $B_0 = 4.0 \times 10^8(Tesla)$ (DotDashed, Blue) with $\varepsilon_0 \approx 3.08$. Other parameters are $T_F \approx 8.68 \times 10^7(^{\circ}K)$, $l_z = 0.99$, $g_Q = 0.0445$, $n_0 \approx 3.0 \times 10^{33}(m^{-3})$ and $H \approx 0.00044$	44
3.3	Profile of Sagdeev potential curves $K(n)$ against number density n using Eq.(3.18) for different values of magnetic field strength such that (i) $B_0 = 3.0 \times 10^7(Tesla)$ (Bold, Black) with $\varepsilon_0 \approx 1.17$. (ii) $B_0 = 6.0 \times 10^7(Tesla)$ (Dashed, Red) with $\varepsilon_0 \approx 2.33$. (iii) $B_0 = 9.0 \times 10^7(Tesla)$ (DotDashed, Blue) with $\varepsilon_0 \approx 3.50$. Other parameters are $n_0 \approx 2.62 \times 10^{32}(m^{-3})$, $T_F \approx 1.72 \times 10^7(^{\circ}K)$, $l_z = \sqrt{1.5}$ and $g_Q = 0.1$	45

- 3.4 Variation of the corresponding solitary wave profiles $\bar{n}(\xi)$ of Figure 3.3 using Eq.(3.20) for different values of spin magnetization energy. All parameters are same as in Figure 3.3. 45
- 4.1 The dip soliton structure (nearly non-degenerate) is plotted between δn and μ for (i) $\xi = 0.92$ (Bold, Black) with $\alpha \approx 0.41$, $n_o \approx 3.5 \times 10^{24} cm^{-3}$ and $T_e \approx 3.7 \times 10^6 K$, (ii) $\xi = 0.94$ (Dashed, Red) with $\alpha \approx 0.31$, $n_o \approx 2.9 \times 10^{24} cm^{-3}$ and $T_e \approx 3.4 \times 10^6 K$ and (iii) $\xi = 0.96$ (DotDashed, Blue) with $\alpha \approx 0.21$, $n_o \approx 2.3 \times 10^{24} cm^{-3}$ and $T_e \approx 3.1 \times 10^6 K$. Other parameters are , $B_0 = 10^{10}G$, $K_x = 0.1$, $M = 1.1$ and $\Lambda = 0.0005$ 56
- 4.2 The dip soliton profile (nearly degenerate) of δn versus μ for $\delta = 0.65$ (Bold, Black) with $\alpha \approx 0.06$, $n_o \approx 4.1 \times 10^{26} cm^{-3}$ and $T_F \approx 2.7 \times 10^7 K$, (ii) $\delta = 0.75$ (Dashed, Red) with $\alpha \approx 0.26$, $n_o \approx 8.0 \times 10^{26} cm^{-3}$ and $T_F \approx 4.1 \times 10^7 K$, and (iii) $\delta = 0.85$ (DotDashed, Blue) with $\alpha \approx 0.86$, $n_o \approx 1.8 \times 10^{27} cm^{-3}$ and $T_F \approx 7.1 \times 10^7 K$. Other parameters are , $B_0 = 10^{11.8}G$, $K_x = 0.1$, $M = 1.1$ and $\Lambda = 0.001$ 57
- 4.3 The hump soliton structure (nearly non-degenerate) is plotted between δn and μ for (i) $\xi = 0.88$ (Bold, Black) with $\alpha \approx 0.99$, $n_o \approx 7.05 \times 10^{23} cm^{-3}$ and $T_e \approx 1.1 \times 10^6 K$, (ii) $\xi = 0.89$ (Dashed, Red) with $\alpha \approx 0.88$, $n_o \approx 6.4 \times 10^{23} cm^{-3}$ and $T_e \approx 1.07 \times 10^6 K$, and (iii) $\xi = 0.90$ (DotDashed, Blue) with $\alpha \approx 0.77$, $n_o \approx 5.9 \times 10^{23} cm^{-3}$ and $T_e \approx 1.04 \times 10^6 K$. Other parameters are , $B_0 = 10^{9.2}G$, $K_x = 0.1$, $M = 0.9$ and $\Lambda = 0.00097$ 58
- 5.1 Sagdeev's potential $K(n)$ is plotted against number density n from Eq.(5.22) for different values of number density (i.e. exchange-correlation), such that (i) $n_0 \approx 1.7 \times 10^{32} m^{-3}$ (Bold) with $g_Q = 0.9$, $T_F \approx 1.3 \times 10^7 (^{\circ}K)$, $\gamma \approx 0.11$, $\lambda \approx 1.18$, $\alpha \approx 0.0006$. (ii) $n_0 \approx 1 \times 10^{33} m^{-3}$ (Dashed) with $g_Q = 0.0.5$, $T_F \approx 4.20 \times 10^7 (^{\circ}K)$, $\gamma \approx 0.06$, $\lambda \approx 1.18$, $\alpha \approx 0.13$. Other parameters are $B_0 = 10^8$, $M = 1.1$, $l_x = 0.3$ 69

5.2	The corresponding dip soliton is plotted between \bar{n} and μ of Figure 5.1 using Eq.(5.40) for different value of number density (i.e. exchange-correlation). All parameters are same as in Figure 5.1.	70
5.3	Profile of Sagdeev's potential curves $K(n)$ against number density n using Eq.(5.22) for different values of magnetic field strength (spin magnetization energy), such that (i) $B_0 = 3 \times 10^7 T$ (Bold) with $\varepsilon_0 \approx 1.5$ and $\alpha \approx 0.07$. (ii) $B_0 = 1 \times 10^8 T$ (Dashed) with $\varepsilon_0 \approx 5.2$ and $\alpha \approx 0.007$. Other parameters are $M = 1.1$, $l_x = 0.3$, $n_0 \approx 1.7 \times 10^{32} m^{-3}$, $T_F \approx 1.3 \times 10^7 (^{\circ}K)$ and $g_Q = 0.9$	70
5.4	The corresponding dip soliton is plotted between \bar{n} and μ of Figure 5.3 using Eq.(5.40) for different values of magnetic field strength (spin magnetization energy). All parameters are same as in Figure 5.3. . . .	71
5.5	Sagdeev's potential $K(n)$ using Eq.(5.22) for different values of magnetic field strength (ε_0) with fixed value of $\gamma \approx 0.11$ and $\lambda \approx 1.18$. All parameters are same as in Figure 5.3.	71
5.6	The corresponding dip soliton using Eq.(5.40) for different values of magnetic field strength (ε_0). All parameters are same as in Figure 5.5. . . .	72

Chapter 1

Introduction

1.1 Plasma Physics

When a neutral gas is subjected to a very high temperature very, the particles of a gas (atoms or molecules) become ionized. Electrons will be stripped off by collision due to the increase in thermal agitation of particles. The gas can also be ionized by bombarding energetic electrons (or ions) or by employing intense electric field or ultraviolet rays (or X-rays) or in other ways etc. The dynamic behavior of ionized gas is dominated by electromagnetic forces acting on free charged particles (i.e. electrons, ions) and behave as a conducting medium. The electrons and ions in ionized gas started interacting with electromagnetic fields and in turn, further, produce electromagnetic fields. The presence of a charged particle in the magnetic field created the Lorentz force which gives rise to many novels and spectacular behavior of plasma. The most important difference between plasma and normal gas is the presence of Coulomb interaction among charged particles, which cannot be ignored to study the dynamics of a plasma.

The term "*plasma*" is a Greek word, giving the meaning of "*something molded or fabricated*". Tonks and Langmuir used the term "*plasma*" in 1929 while studying the characteristics of ionized gas in a tube generated by electric discharge. Plasma medium is considered as the fourth form of matter and it has a significantly different characteristic than solids, liquids, and gases. In all states of matter the important concept is binding energy of particles, (i.e. atoms or molecules), which has certain

values in each state. Moreover, the state of matter can be determined with average kinetic energy per particle. In solid-state, if the average kinetic energy of particles becomes larger to binding energy, than the solid will be changed into the liquid state. Similarly, if the average kinetic energy of particles overcome the van der wall forces by breaking its bonds, then the liquid state will be changed into a gaseous state. Hence, to become a plasma state from gas state, the average kinetic energy of particles must exceed the ionization potential of gas atoms[1, 2].

1.2 Quantum Plasmas

Quantum effects can be observed in solid-state objects (i.e. metals, semiconductors, and nanostructures materials etc.)[3, 4] as well as in astrophysical compact objects (i.e. white dwarf, neutron stars, pulsars, magnetars, and black holes etc.)[5, 6, 7]. The quantum effects in plasma system can no longer be ignored, when the distance $n^{-\frac{1}{3}}$ (i.e. interparticle distance) becomes comparable to wavelength λ_B (i.e. thermal de-Broglie wavelength) such that:

$$n\lambda_B^3 \geq 1. \quad (1.1)$$

Here λ_B representing the spatial extension of the wave function (due to quantum uncertainty) can be written as:

$$\lambda_B = \frac{\hbar}{mv_T}, \quad (1.2)$$

where $\hbar(= \frac{h}{2\pi})$ denotes the scaled plank constant. Moreover, when the Fermi temperature of the plasma system becomes greater than the thermal temperature, quantum effects can be observed. Fermi energy ε_F is related with Fermi temperature T_F can be written as

$$k_B T_F = \varepsilon_F = \frac{\hbar^2}{2m} (3\pi^2 n)^{\frac{2}{3}}, \quad (1.3)$$

It is important to mention here that we use Fermi-Dirac distribution function in-

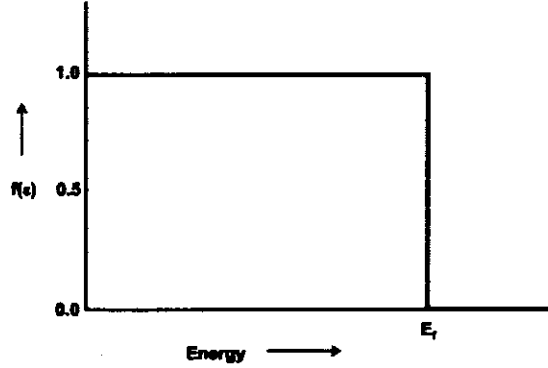


Figure 1.1: $f(\varepsilon)$ at $T_e = 0$

$$(i) \ \varepsilon < \mu, \quad (ii) \ \varepsilon = \mu, \quad (iii) \ \varepsilon > \mu \quad (1.15)$$

Let's see these different cases when $T_e = 0 \text{ K}$. For all $\varepsilon < \mu$, $\frac{\varepsilon - \mu}{k_B T_e}$ tends towards $-\infty$, and hence $f(\varepsilon)$ tends to 1. So, in the limiting case of $T_e = 0 \text{ K}$, we have $f(\varepsilon) = 1$. When $\varepsilon = \mu$, in the limiting case of $T_e = 0 \text{ K}$, $f(\varepsilon)$ is undefined and varies between the two limits 1 and 0. On the other hand, for all $\varepsilon > \mu$, $\frac{\varepsilon - \mu}{k_B T_e}$ tends towards $+\infty$, and hence $f(\varepsilon)$ tends to 0. Figure (1.1) represents $f(\varepsilon)$ at $T_e = 0 \text{ K}$.

Now, we will discuss $f(\varepsilon)$ for values $T_e > 0 \text{ K}$. When we increase the value of thermal temperature, the Fermi-Dirac distribution function $f(\varepsilon)$ varies from 1 to 0. For $\varepsilon = \mu$ at $T_e > 0 \text{ K}$, the term $\frac{\varepsilon - \mu}{k_B T_e} = 0$, and distribution function gives $f(\varepsilon) = 0.5$ regardless of the actual value of the temperature. Similarly, for all $\varepsilon < \mu$, at $T_e > 0 \text{ K}$, the term $\frac{\varepsilon - \mu}{k_B T_e}$ becomes negative and it becomes further negative when the value of ε decreases. It means when ε decreases, the function $f(\varepsilon)$ starts from a value of 0.5 at $\varepsilon = \mu$ and tends towards 1. On the other hand, for all $\varepsilon > \mu$, at $T_e > 0 \text{ K}$, the term $\frac{\varepsilon - \mu}{k_B T_e}$ gives a positive value and it increases when the value of ε increases. Hence, the function $f(\varepsilon)$ starts from a value of 0.5 at $\varepsilon = \mu$ and tends towards 0 as ε increases. This behavior of $f(\varepsilon)$ is summarized in the Figure (1.2).

The normalization constant A in Eq.(1.14) is chosen in such a way that it follows

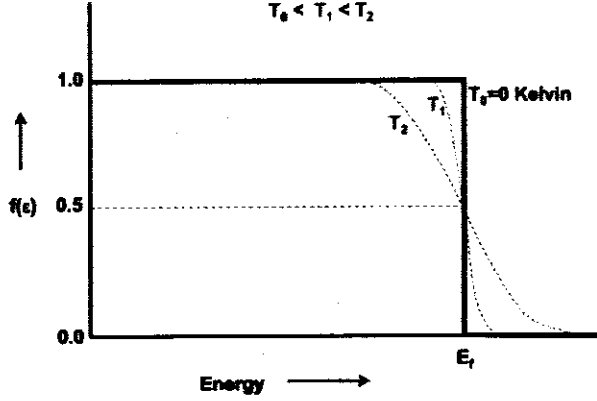


Figure 1.2: $f(\varepsilon)$ at different temperatures.

the Pauli Exclusion Principle, and is given by [3, 4]

$$A = -\frac{n_e}{Li_{\frac{3}{2}}(-e^{\frac{\mu}{k_B T_e}})} \left(\frac{m_e}{2\pi k_B T_e} \right)^{\frac{3}{2}} = 2 \left(\frac{m_e}{2\pi \hbar} \right)^3. \quad (1.16)$$

Where μ and A are supposed to be the functions of time and space with slow variations in the fluid description. Eq.(1.16) contains the polylogarithmic function $Li_v(\zeta)$ of index v which can be generically defined as [11]

$$Li_v(\zeta) = \frac{1}{\Gamma(v)} \int_0^{\infty} \frac{\chi^{v-1}}{\zeta^{-1} e^{\chi} - 1} d\chi, \quad (1.17)$$

where $\chi = \frac{\varepsilon}{k_B T_e}$ and $\zeta = e^{\frac{\mu}{k_B T_e}}$ with $\Gamma(v)$ being the gamma function. FD integral for both density and pressure of degenerate electrons can be expressed as [12]

$$n = \frac{(2m_e k_B T_e)^{\frac{3}{2}}}{2\pi^2 \hbar^3} \int_0^{\infty} \frac{\chi^{\frac{1}{2}} d\chi}{e^{(\chi-\zeta)} + 1}, \quad (1.18)$$

$$p = \frac{2}{3} \frac{(2m_e k_B T_e)^{\frac{5}{2}}}{4m_e \pi^2 \hbar^3} \int_0^{\infty} \frac{\chi^{\frac{3}{2}} d\chi}{e^{(\chi-\zeta)} + 1}. \quad (1.19)$$

Eqs.(1.18) and (1.19) can be expressed in an integral-free form by using polylogarithmic function as [13]

$$n(\mu, T) = -\frac{(2m_e k_B T_e)^{\frac{3}{2}}}{2\pi^2 \hbar^3} \Gamma\left(\frac{3}{2}\right) Li_{\frac{3}{2}}(-\zeta), \quad (1.20)$$

$$p(\mu, T) = -\frac{2}{3} \frac{(2m_e k_B T_e)^{\frac{5}{2}}}{4m_e \pi^2 \hbar^3} \Gamma\left(\frac{5}{2}\right) Li_{\frac{5}{2}}(-\zeta). \quad (1.21)$$

After simplifying Eqs. (1.20) and (1.21), we obtain the expression for pressure in terms of polylogarithm as:

$$p = G n_e k_B T_e. \quad (1.22)$$

This is the barotropic equation of state, where parameter $G = \frac{Li_{\frac{5}{2}}(-\zeta)}{Li_{\frac{3}{2}}(-\zeta)}$ defines the arbitrary degenerate functions [14, 15].

For nearly non-degenerate plasma case, (i.e. $\zeta \ll 1$), the polylogarithmic function can be expanded as

$$G = 1 + \frac{\zeta}{2^{\frac{5}{2}}}. \quad (1.23)$$

Hence, Eq.(1.22) reads

$$p = \left(1 + \frac{\zeta}{2^{\frac{5}{2}}}\right) n_e k_B T_e. \quad (1.24)$$

On the other hand, for nearly degenerate plasma case $\zeta \gg 1$, we have $-Li_\nu(-\zeta) = \frac{(\ln \zeta)^\nu}{\Gamma(\nu+1)}$. So

$$G = \frac{\frac{T_F}{T_e} \left(1 - \frac{\pi^2}{12} \left(\frac{T_e}{T_F}\right)^2\right)}{5/2}. \quad (1.25)$$

Hence, Eq.(1.22) for the case $\zeta \gg 1$ becomes

$$p = \left(\frac{2}{5}\right) \varepsilon_F \left(1 - \frac{\pi^2}{12} \left(\frac{k_B T_e}{\varepsilon_F}\right)^2\right) n_e, \quad (1.26)$$

where $\varepsilon_F = k_B T_F$ represents the Fermi energy.

1.5 Kinetic and Inertial Alfvén Waves

In 1942 Hannes Olof Gösta Alfvén discovered a new mode called the *shear Alfvén wave* in the conducting plasma propagating along the external magnetic field. These modes are the normal modes of magnetohydrodynamic (MHD), involve magnetic per-

turbations, and have characteristic velocities of the order of the Alfvén velocity $v_A = B/\sqrt{\mu_0\rho}$. The dispersion relation of shear Alfvén waves can be written as: $\omega^2 = k_z^2 v_A^2$. Two fluid model of shear Alfvén waves provides three distinct forms depending upon the value of Alfvén velocity v_A^2 with respect to ion and electron thermal velocities. These three situations depend upon the value of plasma β (where plasma β is the ratio of $p_{kinetic} = nk_B T$ to $p_{magnetic} = \frac{B^2}{2\mu_0}$) for any species σ given as below:

$$\beta_\sigma = \frac{nkT_\sigma}{B^2/2\mu_0}. \quad (1.27)$$

If the temperature of electrons and ions are the same, then this subscript σ will not be used. The ratio of ion thermal velocity to Alfvén velocity gives β_i as

$$\frac{v_{Ti}^2}{v_A^2} = \frac{kT_i/m_i}{B^2/nm_i\mu_0} = \beta_i. \quad (1.28)$$

When $v_A \gg v_{Ti}$, then $\beta_i \ll 1$. Hence the magnetic forces are greater in low β plasma than hydrodynamic forces and opposite is true in case of high β plasma. The ratio of electron thermal velocity to Alfvén velocity gives:

$$\frac{v_{Te}^2}{v_A^2} = \frac{kT_e/m_e}{B^2/nm_i\mu_0} = \frac{m_i}{m_e}\beta_e. \quad (1.29)$$

When $\beta_e \gg m_e/m_i$, then $v_{Te}^2 \gg v_A^2$ and for $\beta_e \ll m_e/m_i$ we have $v_{Te}^2 \ll v_A^2$. Hence, shear Alfvén wave physics is different in $\beta_e \ll m_e/m_i$ and $\beta_e \gg m_e/m_i$ regimes, so both the regimes should be investigated separately. Magnetohydrodynamic model oversimplifies these modes by ignoring β dependence[1].

For $\omega/k_z \sim v_A$ the electric field can no longer be considered as curl-free. Similarly, for $\omega/k_z \sim v_A$, the magnetic field lines are not considered rigid rather they become slightly bent. In this case, it is possible to introduced longitudinal potential ψ described by the relation:

$$E_z = -\partial\psi/\partial z, \quad (1.30)$$

while in the case of slow oscillation under consideration, the transverse component of electric field can be taken as curl-free, we can retain the transverse potential ϕ

described by:

$$E_{\perp} = -\nabla\phi. \quad (1.31)$$

By using, these two potentials, we can consider the bending of lines of force but continue to neglect any change in field strength due to compression of the field. For $\psi = \phi$ of course, even the curvature of field disappears. As per our assumption, the thermal velocity of electrons is greater than the phase velocity of wave $\omega/k_z \sim v_A$, the electron reaches equilibrium along the lines of force. Thus, the longitudinal current arises from the small difference in the transverse velocity of electrons and ions[14].

1.6 Theory of Solitons

The study of nonlinear wave phenomenon has gained a great deal of interest and produces exciting description of formation and propagation characteristics. The term soliton represents a wave pulse (i.e. a wave packet) that sustain its identity (i.e. shape) while traveling with constant speed. It is now well known that the solitons are the result of cancellation between nonlinearity and dispersive effects in the system. To study the characteristics of nonlinear plasma phenomenon, the most exhilarating methods are to make use of either reductive perturbation theory[15] or non-perturbation theory[16]. Both techniques (reductive perturbation theory and non-perturbation theory) have been found very important in developing the theory of solitons in plasma dynamics.

1.6.1 Korteweg-de Vries Equation

Although there are several other nonlinear partial differential equations which yield soliton solutions but the most important one among them describing physical systems is the Korteweg-de Vries equation[17] (describing waves on shallow water surfaces) playing a key role in soliton theory.

$$\frac{\partial u}{\partial t} + c \frac{\partial u}{\partial x} + \varepsilon \frac{\partial^3 u}{\partial x^3} + \gamma u \frac{\partial u}{\partial x}, \quad (1.32)$$

where $u(x, t)$, $c = \sqrt{gd}$, $\varepsilon = c\left(\frac{d^2}{6} - \frac{T}{2\rho g}\right)$, $\gamma = \frac{3c}{2d}$, T and ρ represent wave amplitude, wave speed, dispersive parameter, nonlinear parameter, surface tension and water density respectively. If we put $\varepsilon = \gamma = 0$ in Eq.(1.32), we obtained linear equation in the form $u_t + cu_x = 0$ with speed $v = c = \sqrt{gd}$. In general Eq.(1.32) is nonlinear with exact travelling wave solutions

$$u(x, t) = h \sec h^2[k(x - vt)], \quad (1.33)$$

where $k = \sqrt{\frac{\gamma h}{12\varepsilon}}$ shows that waves with high amplitude are narrower. At an appropriate value of the wave speed, the dispersion effects canceled the nonlinearity. The soliton velocity is linked with amplitude by relation

$$v = c + \frac{\gamma h}{3} = \sqrt{gd}(1 + h/2d), \quad (1.34)$$

which is relevant to Russell's empirical results, given in equation $v = \sqrt{g(d+h)}$ to $O(h)$.

1.6.2 Sagdeev's Pseudopotential Method

A non-perturbative approach known as Sagdeev Potential (SP) is derived to study the plasma acoustic waves of arbitrary/large amplitude[13]. Davis et al. used this approach for the investigation of fluid dynamics and later on the same method was named as Sagdeev's potential approach in the context of plasma dynamics.

Sagdeev's potential approach can give an exact solution of the differential equations describing full nonlinearity. To find Sagdeev potential, we introduce a co-moving frame defined by $\xi = x - Vt$, where V is the wave speed. This method can be explained as follow with the simple example of one-dimensional ion-acoustic plasma wave model[14]:

$$\partial_t n_i + \partial_x n_i v_i = 0, \quad (1.35)$$

$$\partial_t v_i + v_i \partial_x v_i = -\partial_x \phi, \quad (1.36)$$

$$n_e = \exp[\phi], \quad (1.37)$$

$$\partial_x^2 \phi = n_e - n_i. \quad (1.38)$$

The set of basic equations (1.35) to (1.38), after simple algebra, can be written in the following form,

$$\frac{1}{2} \left(\frac{d\phi}{d\xi} \right)^2 + V(\phi) = 0, \quad (1.39)$$

where $V(\phi)$ is known as Sagdeev potential. The particle starts at $\phi = 0$ having velocity $\left(\frac{d\phi}{d\xi} \right)$ and bounced back at $\phi = \phi_m$ and again return at position $\phi = 0$. The conditions for the existence of solitary waves are (i) $V(\phi) = 0$ at $\phi = 0$ and $\phi = \phi_m$, (ii) $\left. \frac{dV}{d\phi} \right|_{\phi=0} = 0$ and (iii) $\left. \frac{dV}{d\phi} \right|_{\phi=\phi_m} \neq 0$.

$V(\phi) < 0$ in between $\phi = 0$ and $\phi = \phi_m$. $V(\phi) > 0$ for $\phi > \phi_m$, here ϕ_m represent amplitude of solitons. On the other hand, Sagdeev's equation for astrophysical plasma can be obtained as

$$\frac{1}{2} \left(\frac{dn}{d\xi} \right)^2 + K(n) = 0, \quad (1.40)$$

here $K(n)$ is called Sagdeev potential in case of density (n) variation. The conditions for the existence of nonlinear waves in terms of density are $n = 1$ (for $\phi = 0$) and $n = N$ (for $\phi = \phi_m$). Taylor's expansion can be applied to $K(n)$ near $n = 1$ and $n = N$ to obtain the conditions for the existence of solitary waves.

1.7 Layout of the Thesis

The thesis is based on a theoretical investigation of the linear and nonlinear analysis of kinetic and inertial Alfvén waves in quantum plasma and is divided into five chapters as follow.

In Chapter 1, we have discussed the quantum plasmas, quantum hydrodynamic model, temperature degeneracy, Fermi-Dirac distribution, kinetic and inertial Alfvén

waves, theory of solitons, Korteweg-de Vries equation and Sagdeev's pseudopotential method.

In Chapter 2 we have investigated the arbitrary temperature degeneracy effects on propagation characteristics of KAWs in low- β quantum plasma. Chapter 2 consists of four sections. Section I gives a literature review related with the problem. The set of nonlinear equations for studying an arbitrary amplitude KAWs in a magnetized quantum plasma along with linear dispersion relation and the derivation of Sagdeev potential are presented in Section II. Numerical analysis and discussion are presented in Section III. The conclusion is then given in Section IV.

In Chapter 3 we have studied the propagation characteristics of KAWs in low- β dense quantum plasma with spin magnetization effects. Chapter 3 consists of four sections. In Section I, the literature review is given related to the problem. The set of nonlinear equations for studying an arbitrary amplitude KAWs with linear dispersion relation and the derivation of Sagdeev potential are presented in Section II. Numerical analysis and discussion are presented in Section III. The summary is then given in Section IV.

In Chapter 4 we have discussed the arbitrary temperature degeneracy effect on propagation characteristics of IAWs in intermediate β (i.e. $\alpha \ll 1$ to $\alpha < 1$) quantum plasma. Chapter 4 consists of four sections. Section I describes the literature review related to the problem. The Korteweg-de Vries equation is derived for studying small amplitude IAWs by using the reductive perturbation technique in a magnetized quantum plasma. The set of nonlinear equations with derivation is presented in Section II. Numerical analysis and discussion are presented in Section III. The summary is then given in Section IV.

In Chapter 5 we have investigated the electron exchange-correlation and spin magnetization effects on propagation characteristics of IAWs in low- β quantum plasma (i.e. $\alpha \ll 1$). Chapter 5 consists of four sections. Section I gives the literature review related to the problem. The Sagdeev potential is derived for studying an arbitrary amplitude IAWs whereas, Korteweg- de Vries equation is derived for studying small amplitude IAWs by using reductive perturbation technique in a magnetized quantum

Chapter 2

Kinetic Alfvén waves in quantum plasmas with arbitrary temperature degeneracy

2.1 Introduction

In the near past, quantum plasma has attracted a great deal of interest due to its application in semiconductors devices[1], nano-structures materials[2], ultra-small electronic devices[3] and in ultra-cold plasmas[4]. Quantum effects are also important in laser induced plasmas[5] and in astrophysical compact objects like neutron stars, pulsars, magnetars and interior of white dwarf[6]. When the distance among the particles becomes equal to de-Broglie wavelength and pressure degeneracy becomes equal to classical thermal pressure, then the electron tunneling effects become important in dense plasmas. At high density, due to Pauli exclusion principle, particles follow the Fermi-Dirac distribution function[7, 8, 9, 10]. For degenerate plasmas, equation of state for both non-relativistic and ultra-relativistic was derived by Chandrasekhar [11]. For the case of degenerate electrons, the equation of state is $p_e \propto n_e^{\frac{5}{3}}$ in non-relativistic limit and for ultra-relativistic case, the equation of state is $p_e \propto n_e^{\frac{4}{3}}$, with p_e , n_e are being the degenerate pressure and degenerate electron density respectively.

It is well known that the electrons due to their lower mass are responsible for

quantum effects as compared to heavy ions and follow Fermi-Dirac statistics and the equation of state is obtained from Fermi-Dirac distribution [17, 18]. By using Fermi-Dirac distribution in terms of polylogarithmic function, Melrose et.al. [11, 12] have investigated the degeneracy effects in quantum plasma in addition to quantum recoil effects. They have obtained the longitudinal response function for various sets of electrostatic waves. Maxwell-Boltzmann distribution function will be replaced by a Fermi-Dirac distribution function when we consider temperature degeneracy. In non-degenerate limit, $\frac{\mu}{k_B T_e}$ is large and negative ($\zeta = \exp[\frac{\mu}{k_B T_e}]$) implying $\zeta \rightarrow 0$. In completely degenerate limit, $\frac{\mu}{k_B T_e}$ becomes large and positive, implying $\zeta \rightarrow \infty$, with $\mu_e \rightarrow T_F = \frac{1}{2} m_e v_F^2$, where T_F is the Fermi temperature and v_F is the Fermi speed [11, 12]. By employing a similar approach of Refs. [13, 14], the propagation characteristics of ion-acoustic waves were investigated for nonrelativistic, unmagnetized and magnetized quantum plasma with electrons degeneracy using the fluid model. They further modified the equation of state by deriving the pressure tensor using the Fermi-Dirac statistics [14, 15].

A magnetohydrodynamic model for a quantum magnetoplasma has been derived by Haas [16]. The dynamics of quantum plasma has been studied extensively from these derived equations [16, 17]. By using the quantum magnetohydrodynamic (QMHD) model [18], the tunneling phenomena and negative differential resistance in semiconductor physics can be elaborated. Recently, the phenomena of collective effects in quantum plasma has gained the attention of many researchers [17, 18, 19, 20, 21, 22, 23, 24]. Using QMHD model, many researchers have studied the quantum effects on propagation characteristics of electrostatic and electromagnetic waves [25, 26, 27, 28, 29, 30, 31, 32]. In MHD theory, it is well known that when the perpendicular wavelength to the magnetic field becomes comparable to ion larmor radius, The ions don't follow the magnetic field lines due their heavy mass, whereas the electrons still move along the magnetic field lines due to their small larmor radius. Therefore a charge separation is created due to the small difference of the transverse velocities between ion and electron [17, 18, 21, 22].

Kinetic Alfvén waves are responsible for the acceleration of electrons due to the presence of a strong electric field parallel to the magnetic field. The cancellation of dispersion effects with nonlinearity has resulted in solitary kinetic Alfvén waves (SKAWs) [33,

[54, 55]. In the past, many researchers have investigated the existence of kinetic Alfvén solitons with both density dip and hump traveling obliquely to the direction of an ambient magnetic field in low- β plasma [56, 57, 58, 59, 60]. Moreover, the extensive study on SKAWs was supported by data provided by Freja satellite observation [61, 62]. In the last decade, linear and nonlinear propagation characteristics of kinetic Alfvén waves with finite value of β (i.e., $m_e/m_i < \beta < 1$) as well as inertial Alfvén waves with low β (i.e., $\beta < m_e/m_i < 1$) in electron-positron-ion (EPI) plasmas have been discussed in detail by employing magnetohydrodynamic (MHD) equations owing to its potential applications in astrophysical, laboratory and space environments [63, 64]. They have neglected ion parallel motion but nonlinear density structure is taken into account. Furthermore, their work revealed that the dynamics of KAWs and IAWs can be modified greatly with the inclusion of positrons in electron-ion plasma. Conversely, the inclusion of ions in electron-positron plasmas can change the spatial and temporal scales. Later on, nonlinear low-frequency electromagnetic waves were studied in EPI plasma by taking into account the effects of full nonlinearity and three-dimensional ion motion [65]. The propagation characteristics of low-frequency shear electromagnetic wave in EPI plasma were investigated by Khan [66] with effect of quantum degeneracy, ion correlations and relativistic effects of electrons and positrons. In this study, our objective is to investigate the arbitrary temperature degeneracy effects on propagation characteristics of KAWs in low- β quantum plasma. The set of nonlinear equations for studying an arbitrary amplitude KAWs in a magnetized quantum plasma along with linear dispersion relation and the derivation of Sagdeev potential are presented in Section 2. Numerical analysis and discussion are presented in Section 3. The conclusion is then given in the final section.

2.2 Model Equations

Let's consider a collisionless, homogenous and non-relativistic electron-ion quantum plasma placed in a uniform magnetic field $B = B_0 \hat{z}$ and suppose that the wave is traveling in the $x-z$ plane. To study KAWs in low- β quantum plasma, ions are assumed

to be classical and inertial, whereas the electrons are taken to be degenerate and inertialess. The value of plasma beta $\beta (= 2\mu_0 nk_B T_e / B_0^2)$ is greater than an electron to ion mass ratio but very less than unity such as $\frac{m_e}{m_i} \ll \beta \ll 1$. Due to low- β assumption, one can use two potential theory such that $E_z = -\partial_z \psi$ and $E_x = -\partial_x \varphi$ where ψ and φ are two potentials in longitudinal and transverse direction respectively [67, 68]. The governing equations to study KAWs in dense plasma are given below. The ion continuity and momentum equations are, respectively, given by

$$\partial_t n_i + \partial_x (n_i v_{ix}) = 0, \quad (2.1)$$

$$\frac{d\mathbf{v}_i}{dt} = \frac{e}{m_i} (\mathbf{E} + \mathbf{v} \times \mathbf{B}), \quad (2.2)$$

where v_{ix} represents polarization drift velocity, n_i is the ion number density, m_i is the mass of ion, e is the charge. To avoid vector nonlinearity, the nonlinear term $(v_i \cdot \nabla)$ of convective derivative in Eq.(2.2) can often be neglected. Also in Eq.(2.2) we have also neglected the effects of ion parallel motion along the magnetic field due to low- β assumption. In the limit $|\partial_t| \ll \omega_{ci}$, where $\omega_{ci} (= \frac{eB_0}{m_i})$ is the ion cyclotron frequency, the Eq.(2.2) takes the following form:

$$v_{ix} = -\frac{m_i}{eB_0^2} \partial_t \partial_x \varphi. \quad (2.3)$$

The electron momentum equation is given by:

$$e \partial_z \psi - G k_B T_e \partial_z \ln n_e = 0, \quad (2.4)$$

here $G = \frac{Li_{\frac{5}{2}}(-\zeta)}{Li_{\frac{3}{2}}(-\zeta)}$ defines the arbitrary degenerate functions [7] and will be discussed later. The modified form of Faraday's law ($\partial_x \partial_z (\varphi - \psi) = \partial_t B_y$) for the two potential theory along with Ampere's Law ($\partial_x B_y = \mu_0 J_z$) can be expressed as

$$\partial_x^2 \partial_z^2 (\varphi - \psi) = \mu_0 \partial_t \partial_x J_z, \quad (2.5)$$

here μ_0 is the vacuum magnetic permeability. The quasi-neutrality condition ($n_i \simeq n_e \simeq n$) implies that $\nabla \cdot J = 0$ with

$$\partial_x J_{ix} = -\partial_z J_z, \quad (2.6)$$

where $J_{ix} = e(n_i v_{ix})$, $J_z = -e(n_e v_{ez})$. So, continuity equation reads as

$$\partial_t(en_i) = \partial_z J_z, \quad (2.7)$$

here because of the low- β assumption, the contribution of ions to the current density is negligible; hence J_z is given by the electron density. It is to be noted here that the parallel current due to electrons (i.e. J_z) is cancelled out due to ion polarization current. Eq.(2.7) represents the charge conservation and is identical to Eq.(6) as reported by Ref.[1] for electron-ion classical plasma. For convenience, we use $\xi = \frac{x}{\rho_s}$, $\varsigma = \left(\frac{\omega_{pi}}{c}\right) z$, $\tau = \omega_{ci} t$, $n_i = \frac{n_i}{n_{i0}}$, $\Phi = \frac{e\varphi}{k_B T_e}$, and $\Psi = \frac{e\psi}{k_B T_e}$, here $\rho_s = \left(\frac{T_e}{m_i}\right)^{\frac{1}{2}} \frac{1}{\omega_{ci}}$ is the gyro-radius for ion and $\omega_{pi} = \left(\frac{n_{i0} e^2}{\epsilon_0 m_i}\right)^{\frac{1}{2}}$ is the plasma frequency for ion and T_e is the electron temperature. Also, n_{i0} is the equilibrium number density for ions and the speed of light is denoted by c .

Simplying Eq.(2.3) in dimensionless form as

$$v_{ix} = -\frac{m_i}{eB_0^2} \cdot \frac{\partial_\xi}{\rho_s} \cdot \Omega_i \partial_\tau \cdot \frac{\Phi T_e}{e}, \quad (2.8)$$

$$v_{ix} = -\frac{m_i}{eB_0^2} \cdot \frac{\Omega_i}{\rho_s} \cdot \frac{T_e}{e} \cdot \partial_\xi \partial_\tau \Phi. \quad (2.9)$$

Also, simplying Eq.(2.1) in dimensionless form as

$$\Omega_i \partial_\tau n_i n_{i0} + \frac{\partial_\xi}{\rho_s^2} (n_i n_{i0} v_{ix}), \quad (2.10)$$

$$\Omega_i \partial_\tau n_i - \partial_\xi (n_i \partial_\xi \partial_\tau \Phi) \frac{m_i}{eB_0^2} \cdot \frac{T_e}{e} \cdot \frac{m_i}{T_e} \cdot \frac{e^2 B_0^2}{m_i^2}, \quad (2.11)$$

$$\partial_\tau n_i - \partial_\xi (n_i \partial_\xi \partial_\tau \Phi) = 0. \quad (2.12)$$

Eq.(2.4) in dimensionless form becomes

$$\partial_\xi \Psi = G \partial_\xi \ln n_e. \quad (2.13)$$

Eq.(2.5) can be written in dimensionless form as

$$\frac{\partial_\xi^2}{\rho_s^2} \cdot \frac{\omega_{pi}^2 \partial_\xi^2}{c^2} \cdot \frac{T_e}{e} (\Phi - \Psi) = \Omega_i \mu_0 \partial_\tau \frac{\omega_{pi} \partial_\xi}{c} J_z, \quad (2.14)$$

$$\frac{1}{\rho_s^2} \cdot \frac{\omega_{pi}^2}{c^2} \cdot \frac{T_e}{e} \cdot \partial_\xi^2 \partial_\xi^2 (\Phi - \Psi) = \frac{\mu_0 \Omega_i \omega_{pi}}{c} \partial_\tau \partial_\xi J_z, \quad (2.15)$$

$$\frac{c}{\mu_0 \Omega_i \omega_{pi}} \cdot \frac{1}{\rho_s^2} \cdot \frac{\omega_{pi}^2}{c^2} \cdot \frac{T_e}{e} \cdot \partial_\xi^2 \partial_\xi^2 (\Phi - \Psi) = \partial_\tau \partial_\xi J_z, \quad (2.16)$$

$$\frac{1}{\mu_0 \omega_{pi}} \cdot \frac{\Omega_i n_{i0} e}{c \epsilon_0} \cdot \partial_\xi^2 \partial_\xi^2 (\Phi - \Psi) = \partial_\tau \partial_\xi J_z, \quad (2.17)$$

$$\frac{\Omega_i n_{i0} e c}{\omega_{pi}} \partial_\xi^2 \partial_\xi^2 (\Phi - \Psi) = \partial_\tau \partial_\xi J_z. \quad (2.18)$$

Eq.(2.7) in dimensionless form

$$\frac{\omega_{pi} \partial_\xi J_z}{c} = \Omega_i \partial_\tau (e n_i n_{i0}), \quad (2.19)$$

$$\partial_\xi J_z = \frac{\Omega_i n_{i0} e c}{\omega_{pi}} \partial_\tau n_i. \quad (2.20)$$

Since the parameter $G = \frac{Li_{\frac{5}{2}}(-\zeta)}{Li_{\frac{3}{2}}(-\zeta)}$ defines the arbitrary degenerate functions [4]. For nearly non-degenerate (NND) limit $\zeta \ll 1$, we expand the polylogarithmic function as $Li_\nu(-\zeta) = -\zeta + \frac{(-\zeta)^2}{2^\nu}$ which implies $Li_{\frac{5}{2}}(-\zeta) = -\zeta + \frac{(-\zeta)^2}{2^{\frac{5}{2}}}$ and $Li_{\frac{3}{2}}(-\zeta) = -\zeta + \frac{(-\zeta)^2}{2^{\frac{3}{2}}}$ which makes the value of G as $G_{NND} = (1 + \frac{\zeta}{2^{\frac{1}{2}}})$. Here G_{NND} is arbitrary degeneracy for nearly non-degenerate plasma state. For complete non-degenerate plasma $\zeta \rightarrow 0$

which implicates $G_{NND} = 1$. Similarly for nearly degenerate (ND) limit $\zeta \gg 1$ the polylogarithmic function can be expanded as $-Li_\nu(-\zeta) = \frac{(\ln \zeta)^\nu}{\Gamma(\nu+1)}$ that's implies $Li_{\frac{3}{2}}(-\zeta) = -\frac{(\ln \zeta)^{\frac{3}{2}}}{\Gamma(\frac{7}{2})}$ and $Li_{\frac{5}{2}}(-\zeta) = -\frac{(\ln \zeta)^{\frac{5}{2}}}{\Gamma(\frac{9}{2})}$, the ratio of these terms gives $G_{ND} = (\frac{\ln \zeta}{2})$. Using then the Sommerfeld lemma [35, 36] $\mu = k_B T_F \left[1 - \frac{\pi^2}{12} \left(\frac{T_e}{T_F} \right)^2 \right]$, and hence $\ln \zeta = \frac{T_F}{T_e} - \frac{\pi^2}{12} \frac{T_e}{T_F}$ that implies $G_{ND} = \frac{2}{5} \frac{1}{\delta} \left(1 - \frac{\pi^2}{12} (\delta)^2 \right)$, where G_{ND} represents the arbitrary degeneracy for nearly degenerate plasma with $\delta = \frac{T_e}{T_F}$. For complete degenerate case $\frac{T_e}{T_F} (= \delta) \rightarrow 0$, $\mu \rightarrow T_F = \frac{1}{2} m_e v_F^2$ with T_F and v_F being the Fermi temperature and Fermi speed, respectively.

The ratio of electrostatic interaction energy (i.e. $\langle E_{int} \rangle \approx e^2/4\pi\epsilon_0 r_s$, where r_s is the Wigner-Seitz ratio defined as $r_s = (\frac{3}{4\pi n_0})^{\frac{1}{3}}$) to the average kinetic energy (i.e. $\langle E_{kin} \rangle = (m_e/2n_e) \int f v^2 d^3\nu$, here the scalar pressure $p = \frac{m_e}{3} \int f v^2 d^3\nu$ follows from the standard definition for an equilibrium with zero drift velocity) will give general coupling parameter g covering ND and NND limiting cases in the following form [35, 36].

$$g = \frac{\langle E_{int} \rangle}{\langle E_{kin} \rangle} = \frac{1}{6} \left(\frac{4}{3\pi^2} \right)^{\frac{1}{3}} \frac{e^2 n_0^{\frac{1}{3}} Li_{\frac{3}{2}}(-\zeta)}{\epsilon_0 k_B T_e Li_{\frac{5}{2}}(-\zeta)} \quad (2.21)$$

$$= \frac{\sqrt{m_e/2k_B T_e} e^2 \left(Li_{\frac{3}{2}}(-\zeta) \right)^{\frac{4}{3}}}{3^{\frac{4}{3}} \pi^{\frac{7}{6}} \epsilon_0 \hbar Li_{\frac{5}{2}}(-\zeta)}, \quad (2.22)$$

here ϵ_0 represents permittivity in the vacuum. To fulfill the condition of collisionless plasma, the interaction energy must be lower than kinetic energy such that $g \ll 1$. We have $g \propto \langle E_{int} \rangle / k_B T_e$ for the nearly non-degenerate case and $g \propto \langle E_{int} \rangle / \epsilon_F$ for the nearly degenerate case with ϵ_F being the Fermi energy. Hence, for NND limit $\zeta \ll 1$, we have $Li_\nu(-\zeta) = -\zeta + \frac{(\zeta)^2}{2\nu}$, and Eqs. (2.21) and (2.22) can be written yielding T_e and n_0 .

$$T_e = \frac{m_e}{2k_B \times 3^{\frac{8}{3}} \pi^{\frac{7}{3}}} \left(\frac{e^2}{\epsilon_0 \hbar} \right)^2 \frac{\left(-\zeta + \frac{(\zeta)^2}{2^{\frac{3}{2}}} \right)^{\frac{8}{3}}}{\left(-\zeta + \frac{(\zeta)^2}{2^{\frac{3}{2}}} \right)^2}, \quad (2.23)$$

$$n_0 = \frac{3\pi^2}{4} \left(\frac{6\epsilon_0 k_B T_e}{e^2} \left(1 + \frac{\zeta}{2^{\frac{3}{2}}} \right) \right)^3. \quad (2.24)$$

Similarly for ND case $\zeta \gg 1$, the polylogarithmic function becomes $-Li_\nu(-\zeta) = \frac{(\ln \zeta)^\nu}{\Gamma(\nu+1)}$. So Eqs. (2.21) and (2.22) can be written in the following form yielding the value of ε_F and n_0 .

$$\varepsilon_F = \frac{m_e}{2} \frac{e^2}{3^{\frac{8}{3}} \pi^{\frac{7}{3}} \epsilon_0 \hbar^{\frac{2}{5}} \left(1 - \frac{\pi^2}{12} (\delta)^2\right)} \left(\frac{15\sqrt{\pi}}{8}\right)^2 \left(\frac{4}{3\sqrt{\pi}}\right)^{\frac{8}{3}}, \quad (2.25)$$

$$n_0 = \frac{3\pi^2}{4} \left(\frac{12\epsilon_0}{5e} \varepsilon_F \left(1 - \frac{\pi^2}{12} (\delta)^2\right)\right)^3. \quad (2.26)$$

2.2.1 Linear Wave Analysis

The linear dispersion relation of KAWs in magnetized quantum plasma with arbitrary temperature degeneracy using Eqs.(2.1),(2.4),(2.5) and (2.7) can be written as

$$\omega = k_z V_A \sqrt{1 + k_x^2 G \rho_s^2}. \quad (2.27)$$

Here $\rho_s^2 = \frac{C_s^2}{\omega_{ci}^2}$, $C_s = \sqrt{\frac{k_B T_e}{m_i}}$, and $V_A = \frac{B_0}{\sqrt{\mu_0 m_i n_{i0}}}$ are the gyroradius of ion, acoustic speed and Alfvén velocity respectively. Noting that inertial effects are provided by ions in Eq.(2.27). It is important to mention that the KAWs transports energy slowly in transverse direction for $k_x \gg k_z$. When $\zeta \ll 1$, the dispersion relation for NND limiting case from Eq.(2.27) is

$$\omega = k_z V_A \sqrt{1 + k_x^2 \left(1 + \frac{\zeta}{2^{\frac{5}{2}}}\right) \rho_s^2}. \quad (2.28)$$

If the parameter ζ is ignored in Eq.(2.28) such that $\zeta = 0$, then we have same linear dispersion relation as reported in Ref.[33] for pure classical plasma case. For $\zeta \gg 1$, Eq.(2.27) yields the dispersion relation for ND limiting case as

$$\omega = k_z V_A \sqrt{1 + k_x^2 \frac{2}{5} \frac{1}{\delta} \left(1 - \frac{\pi^2}{12} (\delta)^2\right) \rho_q^2}, \quad (2.29)$$

where $\rho_s = \frac{C_q}{\omega_{ci}}$ and $C_q = \sqrt{\frac{k_B T_F}{m_i}}$ are quantum ion gyro radius and quantum ion acoustic speed. It is be noted here that if we ignore parameter δ in Eq.(2.29) such

that $\frac{T_e}{T_p} (= \delta) \rightarrow 0$ (i.e. for complete degenerate plasma case), then the result will be similar to the dispersion relation reported in Ref.[13] for kinetic Alfvén waves in dense degenerate quantum plasma.

2.2.2 Nonlinear Wave Analysis

To find Sagdeev potential, we introduce a co-moving frame defined by $\eta = K_x \xi + K_z \zeta - \tau$, where K_x and $K_z = \sqrt{1 - K_x^2}$ are the direction cosines. Therefore, the set of Eqs.(2.12)–(2.20) in η frame can be written as

$$-\partial_\eta n_i - K_x \partial_\eta (n_i K_x \partial_\eta \times -\partial_\eta \Phi) = 0, \quad (2.30)$$

$$-\partial_\eta n_i + K_x^2 \partial_\eta^2 (n_i \partial_\eta^2 \Phi) = 0, \quad (2.31)$$

$$\partial_\eta n_i - K_x^2 \partial_\eta (n_i \partial_\eta^2 \Phi) = 0, \quad (2.32)$$

and

$$\partial_\eta \Psi = G \partial_\eta \ln n_e, \quad (2.33)$$

and

$$\frac{\Omega_i n_{i0} e c}{\omega_{pi}} \times K_x^2 \partial_\eta^2 \times K_z^2 \partial_\eta^2 (\Phi - \Psi) = K_z \partial_\eta \times -\partial_\eta J_z, \quad (2.34)$$

$$\frac{\Omega_i n_{i0} e c}{\omega_{pi}} K_x^2 K_z^2 \partial_\eta^4 (\Phi - \Psi) = -K_z \partial_\eta^2 J_z, \quad (2.35)$$

and

$$K_z \partial_\eta J_z = \frac{c \Omega_i}{\omega_{pi}} \times \partial_\eta n_i \times e n_{i0}, \quad (2.36)$$

$$K_z \partial_\eta J_z = \frac{-\Omega_i n_{i0} e c}{\omega_{pi}} \partial_\eta n_i. \quad (2.37)$$

Reducing Eqs.(2.32)–(2.37) to its simplest form as

$$-\partial_\eta n + K_x^2 \partial_\eta n \partial_\eta^2 \Phi = 0, \quad (2.38)$$

now integrate

$$-n + K_x^2 n \partial_\eta^2 \Phi + C = 0, \quad (2.39)$$

Apply the boundary conditions, such as $\eta \rightarrow \pm\infty$, then $\partial_\eta n \rightarrow 0$ and $n \rightarrow 1$.

$$1 - n + K_x^2 n \partial_\eta^2 \Phi = 0, \quad (2.40)$$

$$K_x^2 n \partial_\eta^2 \Phi = n - 1, \quad (2.41)$$

$$\partial_\eta^2 \Phi = \frac{n - 1}{n K_x^2}, \quad (2.42)$$

and

$$\frac{\Omega_i n_{i0} e c}{\omega_{pi}} K_x^2 K_z^2 \partial_\eta^4 (\Phi - \Psi) = -K_z \partial_\eta^2 J_z, \quad (2.43)$$

$$K_x^2 K_z^2 \partial_\eta^4 (\Phi - \Psi) = \partial_\eta^2 n, \quad (2.44)$$

integrate the above expression twice;

$$K_x^2 K_z^2 \partial_\eta^3 (\Phi - \Psi) = \partial_\eta n + C, \quad (2.45)$$

$$K_x^2 K_z^2 \partial_\eta^2 (\Phi - \Psi) = n + C, \quad (2.46)$$

$$\partial_\eta^2 \Phi - \partial_\eta^2 G \ln n = \frac{n - 1}{K_x^2 K_z^2}. \quad (2.47)$$

To obtain above expression we have applied the boundary conditions, such as $\eta \rightarrow \pm\infty$, then $\partial_\eta n \rightarrow 0$ and $n \rightarrow 1$.

Since $\partial_\eta^2 G \ln n = G \left(-\frac{1}{n^2} (\partial_\eta n)^2 + \frac{1}{n} \partial_\eta^2 n \right)$, therefore, Eq.(2.42) with Eq.(2.47) give the following relation:

$$\frac{(n-1)}{nK_x^2} - G \left(-\frac{1}{n^2} (\partial_\eta n)^2 + \frac{1}{n} \partial_\eta^2 n \right) = \frac{(n-1)}{K_x^2 K_z^2}, \quad (2.48)$$

$$\frac{(n-1)}{nK_x^2} - \frac{(n-1)}{K_x^2 K_z^2} = G \left(-\frac{1}{n^2} (\partial_\eta n)^2 + \frac{1}{n} \partial_\eta^2 n \right). \quad (2.49)$$

Multiply Eq.(2.49) with $\frac{1}{n} \partial_\eta n$, we obtain:

$$\left(\left(\frac{1}{n} - \frac{1}{n^2} \right) \frac{1}{K_x^2} - \left(1 - \frac{1}{n} \right) \frac{1}{K_x^2 K_z^2} \right) \partial_\eta n = G \left(-\frac{1}{n^3} (\partial_\eta n)^3 + \frac{1}{n^2} \partial_\eta (\partial_\eta^2 n) \right). \quad (2.50)$$

Eq.(2.49) can be further simplified to obtain the Sagdeev energy integral equation in the following form

$$\frac{1}{2} (\partial_\eta n)^2 + U(n, K_z, G) = 0. \quad (2.51)$$

The second term in Eq.(2.51) is the Sagdeev's potential which is given by

$$U(n, K_z, G) = \frac{n}{G K_x^2 K_z^2} [(n-1)(K_z^2 + n) - n \ln n (K_z^2 + 1)]. \quad (2.52)$$

To derive Eq.(2.51) we applied the boundary conditions, such as $\eta \rightarrow \pm\infty$, then $\partial_\eta n \rightarrow 0$ and $n \rightarrow 1$. If we take degeneracy factor equal to unity (i.e. $G = 1$), the Sagdeev's potential U become identical to the relation reported in Ref.[13]. Eq.(2.51) can be interpreted as the energy integral for a particle of a unit mass oscillating in a potential well $U(n, K_z, G)$, having velocity $\partial_\eta n$ with position n . The conditions for the existence of solitary wave solution of Eq.(2.51) require that (i) $|U(1) = U(n_m) = \partial_n U|_{n=1} = 0$, (ii) $|\partial_n^2 U|_{n=1} < 0$. Using Taylor expansion the Sagdeev's potential $U(n, K_z, G)$ near $n = 1$ can be expressed as

$$\frac{1}{2}(\partial_\eta n)^2 = \frac{M}{2GK_x^2K_z^2}(\delta n)^2 + \frac{M-1}{3GK_x^2K_z^2}(\delta n)^3, \quad (2.53)$$

$$\frac{1}{2}(\partial_\eta n)^2 = A(\delta n)^2 + B(\delta n)^3, \quad (2.54)$$

where $A = \sqrt{\frac{M}{2GK_x^2K_z^2}}$ and $B = \sqrt{\frac{M-1}{3GK_x^2K_z^2}}$, while the assumption made in deriving Eq.(2.54) are $\delta n = n - 1$ and $M = K_z^2 - 1 \ll 1 (M > 0)$.

The soliton solution under the small amplitude perturbation can be obtained by using the expanded form of Eq.(2.54) in Eq.(2.51). Then the solution takes the following form

$$\delta n = \frac{3}{2}M \sec h^2 \left[\sqrt{M(G)^{-1}} \frac{\eta}{2|K_x K_z|} \right]. \quad (2.55)$$

For NND case i.e. $\zeta \ll 1$, the Sagdeev potential and its soliton structure can be expressed as

$$U(n, K_z, G) = \frac{n}{\left(1 + \frac{\zeta}{2}\right) K_x^2 K_z^2} [(n-1)(K_z^2 + n) - n \ln n(K_z^2 + 1)], \quad (2.56)$$

$$\delta n = \frac{3}{2}M \sec h^2 \left[\sqrt{\frac{M}{\left(1 + \frac{\zeta}{2}\right)}} \frac{\eta}{2|K_x K_z|} \right]. \quad (2.57)$$

Whereas, for ND case such that $\zeta \gg 1$, the Sagdeev potential and its soliton structure have the following forms

$$U(n, K_z, G) = \frac{n}{\frac{2}{5}\delta \left(1 - \frac{\pi^2}{12}(\delta)^2\right) K_x^2 K_z^2} [(n-1)(K_z^2 + n) - n \ln n(K_z^2 + 1)], \quad (2.58)$$

$$\delta n = \frac{3}{2}M \sec h^2 \left[\sqrt{\frac{M}{\frac{2}{5}\delta \left(1 - \frac{\pi^2}{12}(\delta)^2\right)}} \frac{\eta}{2|K_x K_z|} \right]. \quad (2.59)$$

2.3 Numerical Analysis and Discussion

In this section, we will discuss the numerical plots for KAWs for NND and ND plasma limits. The value of thermal temperature and plasma density of electron is crucial

TH 23/25

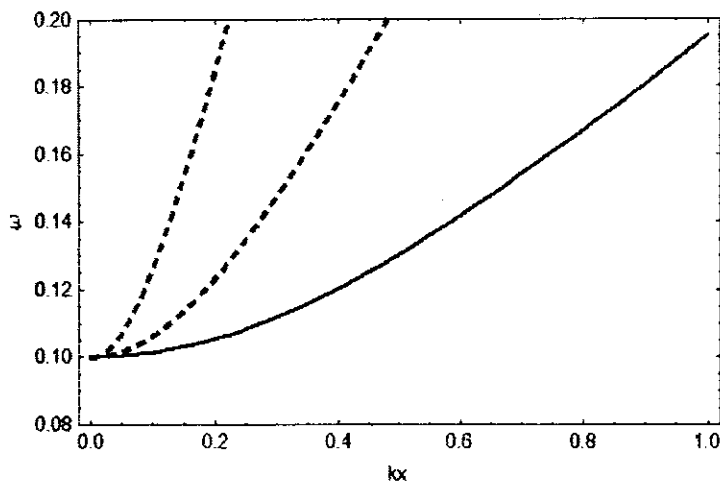


Figure 2.1: Plot of (normalized) frequency ω with respect to (normalized) wavenumber k_x from Eq.(2.28) (nearly non-degenerate plasma) for different values of ζ such that $\zeta = 10^{-4}$ (blue, bold) with $T_e = 2.0 \times 10^4$ ($^{\circ}K$), $n_0 = 1.37 \times 10^{24}$ (m^{-3}), $\zeta = 10^{-3}$ (blue, dashed) with $T_e = 9.2 \times 10^4$ ($^{\circ}K$), $n_0 = 1.37 \times 10^{26}$ (m^{-3}) and $\zeta = 10^{-2}$ (red,dashed) with $T_e = 4.3 \times 10^5$ ($^{\circ}K$), $n_0 = 1.35 \times 10^{28}$ (m^{-3}). Other parameters are $B_0 = 1$ Tesla, $g = 0.1$, $\frac{k_x}{k_0} = 0.1$ and $k_0 = 12500$.

for investigating the ND and NND plasmas limits. So, we have used general coupling parameter g to derive the plasma number density and thermal temperature[23, 24]. To discuss both the NND and ND plasma limiting case for KAWs in quantum plasma, we first plot linear dispersion relation using Eq.(2.28) and Eq.(2.29). Figure (2.1) shows a plot of frequency ω with respect to wavenumber k_x for the NND plasma case by changing the value of ζ . Note that both the frequency ω and wavenumber k_x are normalized such that $\omega = \omega/v_A k_0$, $k_x = k_x/k_0$, here k_0 represent reference wave number. It can be observed from Figure (2.1) that the value of frequency is enhancing with the increase value of parameter ζ for the NND case. On the other hand, Figure (2.2) shows the plot between frequency ω and wavenumber k_x for the ND plasma case for the various value of δ . Again note that both the frequency ω as well as wavenumber k_x are normalized. It is found from Figure (2.2) that the value of frequency reduces by enhancing the value of parameter δ . The plots are shown in Figure (2.1) and Figure (2.2) are identical in trend and nomenclature with the plots reported in Ref. [?].

The effects on Sagdeev potential curve and solitary structure by changing the values of parameter ζ for NND plasma case and δ for ND plasma case for KAWs are shown in

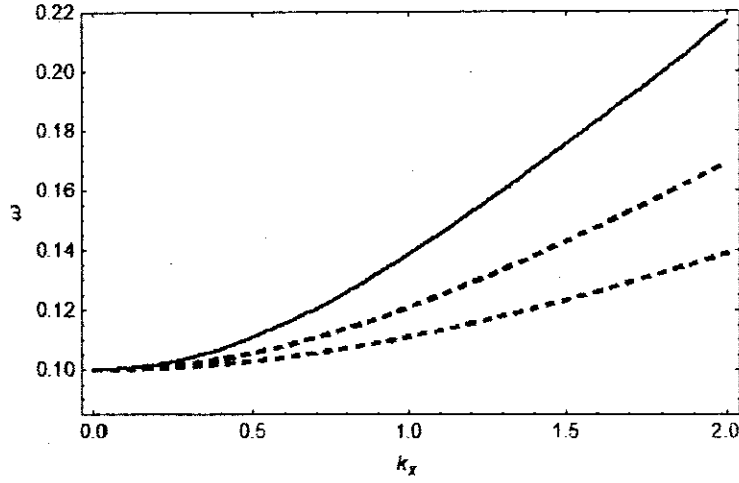


Figure 2.2: The (normalized) frequency ω is plotted against (normalized) wavenumber k_x from Eq.(2.29) (nearly degenerate plasma) for different values of δ such that $\delta = 10^{-4}$ (blue,bold) with $T_F = 4.78 \times 10^7$ ($^{\circ}K$), $T_e = 4780$ ($^{\circ}K$), $n_0 = 1.21 \times 10^{33}$ (m^{-3}), $\delta = 10^{-3.7}$ (blue,dashed) with $T_F = 4.78 \times 10^7$ ($^{\circ}K$), $T_e = 9538.13$ ($^{\circ}K$), $n_0 = 1.21 \times 10^{33}m^{-3}$ and $\delta = 10^{-3.4}$ (red,dashed) with $T_F = 4.78 \times 10^7$ ($^{\circ}K$), $T_e = 19031.1$ ($^{\circ}K$), $n_0 = 1.21 \times 10^{33}$ (m^{-3}). Other parameters are $B_0 = 5.4 \times 10^3$ Tesla, $g = 0.1$, $\frac{k_z}{k_0} = 0.1$ and $k_0 = 12500$.

Figures (2.3-2.6). The profile of Sagdeev potential U for different value of ζ for NND plasma case from Eq.(2.56) are shown in Figure (2.3). It is found from Figure (2.3) that by increasing the value of parameter ζ for NND plasma case, the depth (width) of Sagdeev potential curves are decreasing while the crossing point (i.e. amplitude) will remain the same. The corresponding soliton structure of Figure (2.3) is shown in Figure (2.4) from Eq.(2.57) for NND plasma case. It is evident from Figure (2.4) that the width of dip soliton is slightly changed by enhancing the value of parameter ζ while no change observed in amplitude. It can be observed from Figure (2.3) that the Sagdeev potential curve gives hump soliton in the sub-Alfvénic region under condition $n_m > n > 1$. This kind of soliton in the sub-Alfvénic region is reported in Ref.[46].

On the other hand, the Sagdeev potential curves U and the corresponding soliton structure for different values of parameter δ for ND plasma case are shown in Figure (2.5) and Figure (2.6) respectively. It is to be noted from Figure (2.5) that the Sagdeev potential curve under condition $1 > n > n_m$ can form hump soliton in the sub-Alfvénic region. It is further found that by increasing the value of parameter δ the depth (width) of Sagdeev potential curves are increasing while the crossing point n_m (i.e. amplitude)

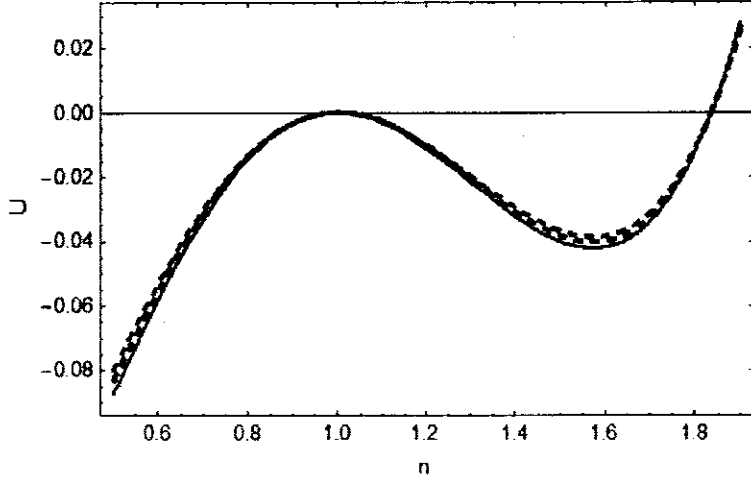


Figure 2.3: Plots of Sagdeev potential U from Eq.(2.56) against number density n for different values of ζ such that $\zeta = 0.1$ (blue, bold) with $T_e = 1.9 \times 10^6$ ($^{\circ}K$), $n_0 = 1.21 \times 10^{30}$ (m^{-3}), $\zeta = 0.45$ (blue, dashed) with $T_e = 4.3 \times 10^6$ ($^{\circ}K$), $n_0 = 1.72 \times 10^{31}$ (m^{-3}) and $\zeta = 0.8$ (red, dashed) with $T_e = 5.5 \times 10^6$ ($^{\circ}K$), $n_0 = 4.08 \times 10^{31}$ (m^{-3}) for nearly non-degenerate plasma limit, while keeping $K_z = \sqrt{1.5}$ and $K_x = \sqrt{1 - K_z^2}$, with $g = 0.1$.

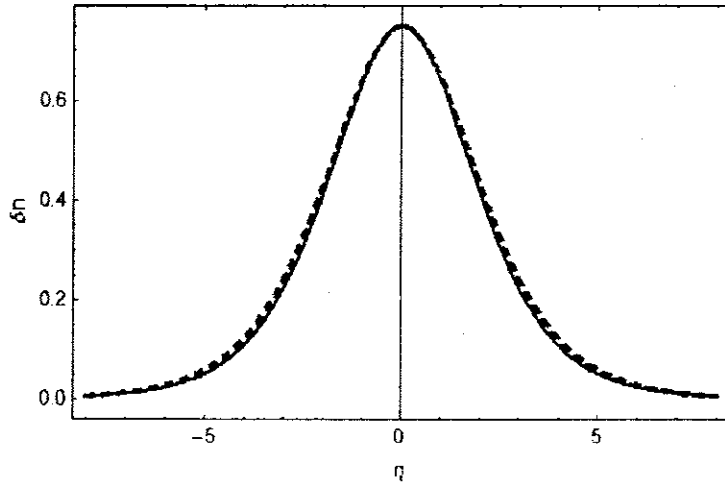


Figure 2.4: Variation of soliton structure of δn versus η from Eq.(2.57) for nearly non-degenerate plasma. All parameters are the same as in Fig. 2.3.

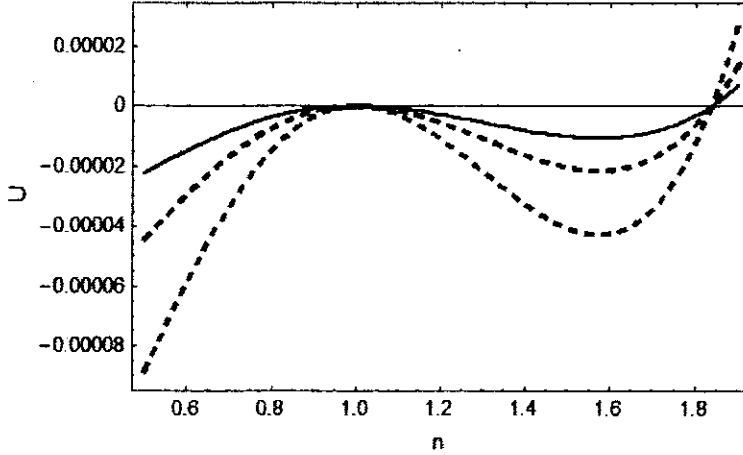


Figure 2.5: Sagdeev potential U is plotted against number density n from Eq.(2.58) for nearly degenerate plasma with same values of δ as in Figure 2.2, while keeping $K_z = \sqrt{1.5}$ and $K_x = \sqrt{1 - K_z^2}$, with $g = 0.1$.

will remain the same. The corresponding soliton structure of Figure (2.5) is shown in Figure (2.6). It is clear from Figure (2.6) that the width of soliton is narrowing by enhancing the value of parameter δ while no change observed in amplitude. Noting that the trend and nomenclature of Figure (2.5) and Figure (2.6) are opposite to Figure (2.3) and Figure (2.4).

From graphical analysis, it is revealed that the Sagdeev potential plot is only possible in the sub-Alfvén region if we consider the value of K_z greater than unity such that $K_z^2 > 1$. Its mean that the solitary wave can not exist in the super Alfvénic region when the value of K_z is less than unity such as $K_z^2 < 1$. So, it is clear from Figures (2.3-2.6) that we have only one kind of soliton solution and the KAWs can only form hump soliton in the sub-Alfvénic region for value $K_z^2 > 1$. It is also found from our numerical analysis that the variation found for Sagdeev potential and soliton structure in the case of ND plasma state is more prominent than the variation observed for Sagdeev potential and soliton structure in case of NND plasma state. Furthermore, If we ignore the quantum effects (i.e. arbitrary temperature degeneracy effects) in terms of NND (i.e. $\zeta = 0$) and ND (i.e. $\delta = 0$) plasma limiting case then the result will be similar as reported in Ref.[3] which is purely for classical plasma case. It is also worth mentioning that our model allow only values $\zeta \leq 1$ for the NND plasma case and $\delta \leq 1$ for the ND plasma case.

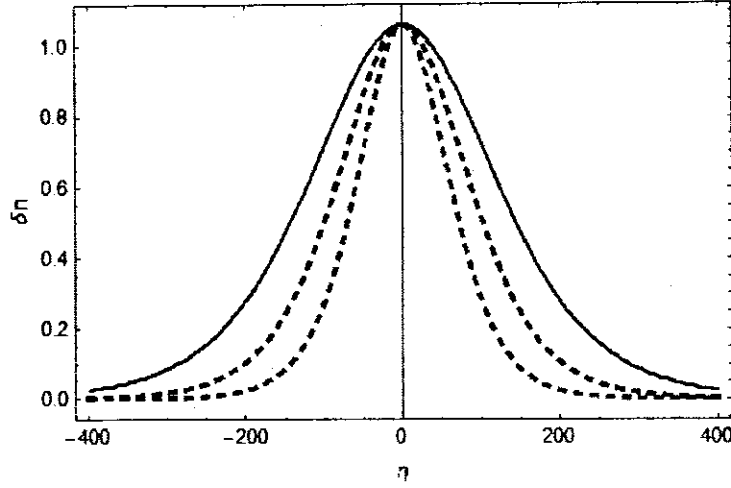


Figure 2.6: The soliton profile of δn versus η from Eq.(2.59) for nearly degenerate plasma. All parameters are the same as in Figure 2.5.

2.4 Conclusion

We have investigated the nonlinear propagation characteristics of kinetic Alfvén waves in low- β quantum plasmas by taking into account arbitrary temperature effects in terms of NND and ND plasma limiting case. The Sagdeev potential was derived by using two potential approximation. It is found that kinetic Alfvén hump solitons exist in both NND and ND plasma limiting case. Furthermore, the kinetic Alfvén hump soliton moves with sub-Alfvénic wave speed. It is observed that the changes in Sagdeev's potential curves and soliton structures in the case of the ND plasma state are more significant than the changes observed for Sagdeev's potential and soliton structure in the case of NND plasma state. Moreover, If we neglect the quantum effects such as arbitrary temperature degeneracy effects for both NND and ND plasma limiting case (i.e. $\zeta = \delta = 0$) than the result will be similar as reported in Ref.[33] for electron-ion classical plasma. Our model with values $\zeta \leq 1$ is only applicable for the NND plasma case and $\delta \leq 1$ for the ND plasma case. Our results may be useful in studying the structure of astrophysical compact objects like white dwarfs, magnetars and pulsars.

Chapter 3

The effect of spin magnetization on Kinetic Alfvén waves in dense plasmas

3.1 Introduction

In 1942 Hannes Alfvén investigated that the low-frequency electromagnetic waves can propagate in conducting fluids such as plasmas by assuming the plasma medium to be a highly conducting, magnetized and incompressible fluid. He discovered a new mode called the shear or torsional Alfvén wave in the conducting plasma propagating along the magnetic field direction. Alfvén waves also known as electromagnetic hydrodynamic waves are ubiquitous. In nature, these types of waves become important in solar physics because the sun has a general magnetic field as well as conducting solar matter. So, Alfvén waves are present everywhere in the universe where there is a magnetic field and conducting fluid and is a normal mode of magnetized plasma. In addition to the shear Alfvén wave, we have fast and slow magnetoacoustic waves for compressible plasma cases. Both kinds of low-frequency wave modes (i.e. Alfvén and magnetoacoustic waves) have gained much attention because they play important roles in the heating of, and the transport of energy in, laboratory, space, and astrophysical plasmas.

The Alfvén waves are found to be the main source of heating of the solar and

stellar coronae as well as a supplementary heating scheme for fusion plasma devices both theoretically and experimentally. The dispersion relation of shear Alfvén waves in uniform plasma is modified greatly due to large perpendicular wavenumber. So, in other words, when the wavelength perpendicular to background magnetic field is short or wavevector is almost perpendicular to the magnetic field and the phase front is parallel to the field, we have different dispersion relations with respect to shear Alfvén dispersion relation. Shear Alfvén waves can be further categorized into kinetic Alfvén waves (KAWs) for warm plasmas and inertial Alfvén waves (IAWs) for cold plasmas depending upon the value of plasma β .

It is revealed from analyzing and studying the data taken by Freja spacecraft that the auroral low-frequency turbulence exhibits strong electromagnetic spikes. From these electromagnetic spikes, the existence of solitary waves with strong density perturbations is observed which reasonably well interpreted as solitary KAWs. The observation by Freja satellite showed KAWs with density depression and hump type structures [1, 2, 3]. KAWs become solitary kinetic Alfvén waves when dispersion canceled out with nonlinearity. Many researchers in the past have studied in detail solitary KAWs especially in classical regime [4, 5, 6, 7]. The classical plasmas exhibit low density and high temperature. It follows Boltzmann-Maxwellian distribution function. The value of de-Broglie is so low in classical plasma that the particles behave like point-like and obey Newtonian mechanics with no overlapping of wave functions. Examples of classical plasma can be found in solar wind, magnetosphere, and ionosphere etc.

The discovery of pulsars have proven the existence of neutrons stars having masses similar to the sun but radii of about $10km$. It is assumed that the neutron stars are the remanent of supernova explosion. The black holes are assumed to be present in certain binary stars system, possibly at the centers of every galaxy and considered as the energy sources in quasi-stellar objects. The majority of stars including our sun will finally evolve as white dwarfs, possessing the same mass as neutron stars but size of the order of earth with interior densities $\sim 10^6 gcm^{-3}$. The evolution of white dwarf is dominant mechanism in galaxies, which is a great source of information in the evolution

of individual stars from birth to death, on the history of galaxies and the rate of star formation. The basic parameter which determines the final fate of a star is thought to be its mass at its birth.

It is believed that all stars with masses in the range 6 to 8 solar masses (i.e. M_{\odot}) will finally become white dwarf, while the more massive stars will become neutron stars or black hole. The maximum mass, a white dwarf can have is $1.4M_{\odot}$, which is a very small fraction of the original stellar mass. The remaining part of the original star is believed to be converted into the surrounding interstellar medium which may be further utilized in the formation of new stars. By calculating the mass of white dwarfs and tracing their evolution to their progenitors, it is possible to find out the total mass loss, at least in a statistical sense.

Recently, there has been a great deal of interest in excitations of collective modes in the spin system, such as spin waves. By employing quantum theory, the study of charged particles and plasmas has gained much attention in astrophysical environments (e.g. strongly magnetized plasmas) [1]. It is also observed that the properties of low-frequency electromagnetic waves in highly magnetized plasmas are significantly modified by the spin effects [2, 3]. Marklund et al. have studied the characteristics of nonlinear magnetosonic waves in strongly magnetized quantum plasma with quantum Bohm potential and electron spin-1/2 effects. In the quantum momentum equation, an additional negative pressure like term was added due to spin effects, as a result, the nonlinear waves become wider and have shallower density depletions for a larger value of magnetization energy (i.e. Zeeman energy) $\varepsilon_0 = \mu_B B / k_B T_e$. The spin of the electrons collectively modifies the quantum dynamics of the MHD plasma [4].

The effects of Bohm potential and spin magnetization on nonlinear magnetosonic waves with shock waves in quantum plasma were studied by Mushtaq and Vladimirov [5]. The effect of Fermi pressure, Bohm potential and spin magnetization on arbitrary nonlinear magnetosonic waves in degenerate plasmas was further investigated by Ref. [6]. Later on, the work was further extended by Mushtaq et al. [7] while studying the characteristics of degenerate electron-positron-ion (EPI) plasmas and found changes in the propagation characteristics of magnetoacoustic waves by changing the value

of positron concentration. Similarly, Maroof et al.[] have investigated the spin-1/2 effects on dispersion properties of magnetoacoustic waves in relativistic degenerate EPI magnetoplasma. Thus, in this study, we investigate the propagation characteristics of KAWs in low- β dense quantum plasma with spin magnetization effects. The set of nonlinear equations for studying an arbitrary amplitude KAWs with linear dispersion relation and the derivation of Sagdeev potential are presented in Section 2. Numerical analysis and discussion are presented in Section 3. The conclusion is then given in the final section.

3.2 Formulation

Let's consider a collisionless, homogenous and non-relativistic low- β electron-ion quantum plasma with effect of spin magnetization placed in a uniform magnetic field $B_0 = B_0 \hat{z}$ and suppose that the wave is traveling in the $x - z$ plane. To study KAWs in low- β quantum plasma, ions are assumed to be classical and inertial, whereas the electrons are taken to be degenerate and inertialess. The value of plasma beta ($\beta = 2\mu_0 n k_B T_{Fe} / B_0^2$) is greater than an electron to ion mass ratio but very less than unity. Due to low- β assumption, one can use two potential theory such that $E_z = -\frac{\partial\psi}{\partial z}$ and $E_x = -\frac{\partial\phi}{\partial x}$ where ψ and ϕ are two potentials in longitudinal and transverse direction respectively[,]. The governing equations to study KAWs in dense quantum plasma are given below. The electron momentum equation is given by[,]

$$\frac{e}{m_e} \frac{\partial\psi}{\partial z} - \frac{1}{m_e n_e} \frac{\partial p_{Fe}}{\partial z} + \frac{\hbar^2}{6m_e^2} \frac{\partial}{\partial z} \left(\frac{\partial^2}{\partial z^2} \sqrt{n_e} \right) + \frac{2\mu_B}{m_e \hbar} \frac{\partial}{\partial z} (\mathbf{S} \cdot \mathbf{B}) = 0, \quad (3.1)$$

here e is the charge, m_e is the mass, n_e (n_i) is the electron (ion) density respectively. Fermi pressure $p_{Fe}(= \frac{m_e v_{Fe}^2}{3n_0^2} n_e^3)$ is shown in second term of Eq.(3.1) with $v_{Fe}(= \sqrt{2k_B T_{Fe}/m_e})$ and $T_{Fe}(= \hbar^2(3\pi^2 n_0)^{2/3}/2m_e k_B)$. Here k_B , \hbar and n_0 are the Boltzmann constant, Plank's constant and equilibrium density (defined as $n_0 = n_{i0} = n_{e0}$). Bohm potential term also called quantum diffraction is shown as third term in Eq.(3.1) The last term of Eq.(3.1) shows spin force . Here μ_B represents Bohr magneton (i.e. $\mu_B = \frac{e\hbar}{2m_e}$) and for the lowest order spin analysis, $S = -\frac{\hbar \mathbf{M}}{2\mu_B n_e}$, with magnetization

vector $M = \left(\frac{n_e \mu_B^2}{\epsilon_F \epsilon} \right) B [\hat{y}, \hat{z}]$. The ion momentum equation is given as

$$\frac{dv_i}{dt} = \frac{e}{m_i} (\mathbf{E} + \mathbf{v}_i \times \mathbf{B}), \quad (3.2)$$

where v_i , n_i , and m_i represent the ion fluid velocity, ion number density, and ion mass respectively. Here $\frac{d}{dt} = \partial_t + v_i \cdot \nabla$ is called convective derivative. In the limit $|\partial_t| \ll \omega_{ci}$, where $\omega_{ci} (= \frac{eB_0}{m_i})$ is the ion cyclotron frequency, the Eq.(3.2) takes the following form

$$v_i = -\frac{1}{B_0 \omega_{ci}} \frac{\partial^2 \phi}{\partial t \partial x}, \quad (3.3)$$

To avoid vector nonlinearity, the nonlinear term $(v_i \cdot \nabla)$ of convective derivative in Eq.(3.2) can often be neglected. The ion continuity equation is

$$\frac{\partial n_i}{\partial t} + \frac{\partial}{\partial x} (n_i v_i) = 0, \quad (3.4)$$

Faraday's law $\nabla \times \mathbf{E} = -\partial_t \mathbf{B}$ can be written as

$$\frac{\partial^2}{\partial x \partial z} (\phi - \psi) = \frac{\partial}{\partial t} B_y, \quad (3.5)$$

Ampere's law can be expressed as

$$\nabla \times \mathbf{B} = \mu_o \mathbf{J}_t + \mu_o \epsilon_o \partial_t \mathbf{E}, \quad (3.6)$$

where $J_t = J_p + J_M$ is the total current density, J_p is the polarization current density, $J_M = \nabla \times M$ is the electron spin magnetization current density and M represent the spin magnetization density. We have ignored the displacement current in above Eq.(3.6). In this case we may write Eq.(3.6) as

$$\nabla \times \mathbf{B} = \mu_o \mathbf{J}_t \Rightarrow \frac{\partial}{\partial x} B_y = \mu_o J_t, \quad (3.7)$$

The quasi-neutrality condition $n_i \simeq n_e \simeq n$ implies that $\nabla \cdot \mathbf{J} = 0$, and further depicts

$$\frac{\partial}{\partial x} J_{ix} = -\frac{\partial}{\partial z} J_t, \quad (3.8)$$

with $J_{iz} = e(n_i \mathbf{v}_{pi})$. Thus, continuity equation becomes

$$\frac{\partial}{\partial t}(en_e) = \frac{\partial}{\partial z} J_t, \quad (3.9)$$

It is to be noted here that current density J_t is mainly resulted due to presence of electrons density as compared to ion density in low- β quantum plasma case. Noting further that electron parallel current and ion polarization current will cancel each other. For convenience, we define the dimensionless parameters as,

$$\epsilon = \frac{x}{\rho_q}, \mu = \left(\frac{\omega_{pi}}{c}\right) z, \tau = \omega_{ci} t, n_{i,e} = \frac{n_{i,e}}{n_o}, \Phi = \frac{e\phi}{k_B T_{Fe}}, \Psi = \frac{e\psi}{k_B T_{Fe}},$$

where ρ_q represents quantum ion gyro-radius such that $\rho_q = C_q/\omega_{ci}$, C_q denotes quantum ion acoustic speed such that $C_q = \sqrt{\frac{k_B T_{Fe}}{m_i}}$, ω_{pi} denotes ion plasma frequency i.e. $\omega_{pi} = \left(\frac{n_{io} e^2}{\epsilon_0 m_i}\right)^{\frac{1}{2}}$ and c means light speed. For convenience, Eqs.(3.1-3.9) can be written in dimensionless form as follow

$$\frac{\partial n}{\partial \tau} - \frac{\partial}{\partial \epsilon} \left(n \frac{\partial^2 \Phi}{\partial \epsilon \partial \tau} \right) = 0, \quad (3.10)$$

$$\frac{\partial \Psi}{\partial \mu} - \frac{1}{2} \frac{\partial n^2}{\partial \mu} + \frac{H^2}{2} \frac{\partial}{\partial \mu} \left(\frac{\partial^2 \sqrt{n}}{\partial \mu^2} \right) - \epsilon_o^2 \frac{\partial}{\partial \mu} \ln n = 0, \quad (3.11)$$

$$\frac{\partial^4}{\partial \epsilon^2 \partial \mu^2} (\Phi - \Psi) = \frac{\partial^2}{\partial \tau^2} n. \quad (3.12)$$

In the above representations, $H = \frac{\hbar \omega_{pi}}{\sqrt{3 m_e c^2 \epsilon_{Fe}}}$ is a dimensionless parameter, shows the Bohm potential effect while $\epsilon_o = \frac{\mu_B B_o}{\epsilon_{Fe}}$ shows the normalized Zeeman energy due to the presence of spin magnetization. The ratio of interaction energy $E_{int} = e^2/4\pi\epsilon_0 (3/4\pi n_0)^{\frac{1}{3}}$ (here ϵ_0 is vacuum permittivity) and Fermi energy $E_F = \frac{\hbar^2}{2m} (3n_0\pi^2)^{\frac{2}{3}}$ gives quantum coupling parameter $g_Q = E_{int}/E_F$. When the value of quantum coupling parameter of dense quantum plasma is less than unity, then we will have collisionless state (i.e. $g_Q \approx 0.64 \times 10^{10} n_0^{-\frac{1}{3}}$) along with plasma density $n_0 \geq 3 \times 10^{29} (m^{-3})$ [].

The linear dispersion relation of KAWs in magnetized quantum plasma with effect of electron spin magnetization and Bohm potential using Eqs.(3.1–3.9) can be written

as follow

$$\omega^2 = k_z^2 V_A^2 \left[1 + k_x^2 \rho_q^2 \left(1 + \varepsilon_o^2 + \frac{H^2 \lambda_i^2 k_z^2}{2} \right) \right], \quad (3.13)$$

where $k_x(k_z)$, $V_A = \frac{B_0}{\sqrt{\mu_0 m_i n_{i0}}}$, and $\lambda_i = c/\omega_{pi}$ represent wave numbers along x -axis (z -axis), velocity of Alfvén wave, and ion Fermi wavelength. If we ignore both the spin and quantum diffraction terms we obtained same result for dispersion relation as reported by Ref.[] in case of pure classical plasma.

Now, we introduce a co-moving frame defined by $\xi = l_x \varepsilon + l_z \mu - \tau$ (where l_x , and $l_z = \sqrt{1 - l_x^2}$ are the direction cosines) to derive the Sagdeev potential equation. Therefore, the set of Eqs.(3.10-3.12) in ξ frame can be written as

$$\frac{\partial}{\partial \xi} n - l_x^2 \frac{\partial}{\partial \xi} \left(n \frac{\partial^2}{\partial \xi^2} \Phi \right) = 0, \quad (3.14)$$

$$\frac{\partial \Psi}{\partial \xi} - n \frac{\partial n}{\partial \xi} - \varepsilon_o^2 \frac{\partial}{\partial \xi} \ln n = 0, \quad (3.15)$$

$$l_x^2 l_z^2 \frac{\partial^4}{\partial \xi^4} (\Phi - \Psi) = \frac{\partial^2}{\partial \xi^2} n. \quad (3.16)$$

Noting that we have ignored the Bohm potential term in Eq.(3.11). Simplifying Eqs.(3.14-3.16) to obtain the Sagdeev energy integral equation in the following form

$$\frac{1}{2} \left(\frac{\partial n}{\partial \xi} \right)^2 + K(n, \varepsilon_o) = 0, \quad (3.17)$$

where $K(n, H, \varepsilon_o)$ is the Sagdeev's potential for this particular problem and is given as

$$K(n, \varepsilon_o) = -\frac{n^2}{(\varepsilon_o + n^2)^2} \left(\begin{aligned} & \frac{n^2}{2 l_x^2} + \frac{\varepsilon_o^2}{n l_x^2} + \frac{\varepsilon_o^2 \ln n}{l_x^2} - \frac{n}{l_x^2} + \frac{n^2}{2 l_x^2 l_z^2} - \frac{n^3}{3 l_x^2 l_z^2} - \frac{n \varepsilon_o^2}{l_x^2 l_z^2} + \frac{\varepsilon_o^2 \ln n}{l_x^2 l_z^2} \\ & - \frac{1}{6 l_x^2 l_z^2} + \frac{\varepsilon_o^2}{l_x^2 l_z^2} + \frac{1}{2 l_x^2} - \frac{\varepsilon_o^2}{l_x^2} \end{aligned} \right). \quad (3.18)$$

In deriving Eq.(3.17) we used boundary conditions such as $\xi \rightarrow \pm\infty, n \rightarrow 1$. Eq.(3.17) can be interpreted as energy integral equation of a particle of unit mass having velocity $\frac{\partial n}{\partial \xi}$ with position n in potential well $K(n, \varepsilon_o)$. The conditions for the existence of

solitary wave solution are (i) $K(n, \varepsilon_o) = 0$ at $n = 1$ and $n = n_m$, (ii) $\frac{\partial K}{\partial n} |_{n=1} = 0$ and $\frac{\partial^2 K}{\partial n^2} |_{n=1} < 0$ and (iii) $K(n, \varepsilon_o) < 0$.

Using Taylor expansion the Sagdeev potential $K(n, \varepsilon_o)$ near $n \approx 1$ can be expressed as

$$\frac{1}{2} \left(\frac{\partial n}{\partial \xi} \right)^2 = A(\bar{n})^2 + B(\bar{n})^3, \quad (3.19)$$

here $A = \sqrt{\frac{l_z^2 - 1}{2l_z^2 l_z^2 (1 + \varepsilon_o)}}$, $B = \sqrt{\frac{2 - 3l_z^2 - 2\varepsilon_o + l_z^2 \varepsilon_o}{3l_z^2 l_z^2 (1 + \varepsilon_o)^2}}$ with $\bar{n} = n - 1$. The soliton solution under the small amplitude perturbation can be obtained by using the expanded form of Eq.(3.19) in Eq.(3.17). Then the solution takes the following form

$$\bar{n} = \lambda \sec h^2 \Delta \xi, \quad (3.20)$$

here $\lambda = \frac{3(1-l_z^2)(1+\varepsilon_o)}{4+2l_z^2(\varepsilon_o-3)-4\varepsilon_o}$ represents the amplitude and $\Delta = \frac{1}{2l_z l_z} \sqrt{\frac{(l_z^2-1)}{(1+\varepsilon_o)}}$ is the width of a solitary wave.

3.3 Numerical Analysis and Discussion

Dense plasmas existing in astrophysical compact stars such as white dwarfs, pulsars and magnetars are characterized by strong magnetic fields $B \approx 10^6 - 10^9 \text{ Tesla}$ [, ,], whereas the plasma number densities are thought to have $n_0 \approx (10^{30} - 10^{35}) m^{-3}$ [, ,]. To study solitary KAWs numerically in a low- β quantum plasma, we have used plasma parameters (in MKS units) $n_0 \approx (10^{32} - 10^{35}) m^{-3}$, $B_0 \approx (10^5 - 10^9) \text{ Tesla}$ and $T_F \approx (10^7 - 10^9) \text{ K}$. Numerically, the magnetization energy can be written as $\varepsilon_0 \approx \varepsilon_0 \approx 1.6 \times 10^{14} \left(B_0/n_0^{\frac{2}{3}} \right)$. It can easily observed that the normalized Zeeman energy ε_0 (due to the spin magnetization) depends on both magnetic field strength and plasma number density.

Now we present the numerical analysis of Eqs.(3.13), (3.18) and(3.20) by changing the values of magnetic field (i.e. ε_0) in Figures (3.1-3.4). We first plot linear dispersion relation using Eq.(3.13) to discuss both the effect of spin magnetization and Bohm potential on KAWs in dense quantum plasma. Figure (3.1) shows a plot of frequency

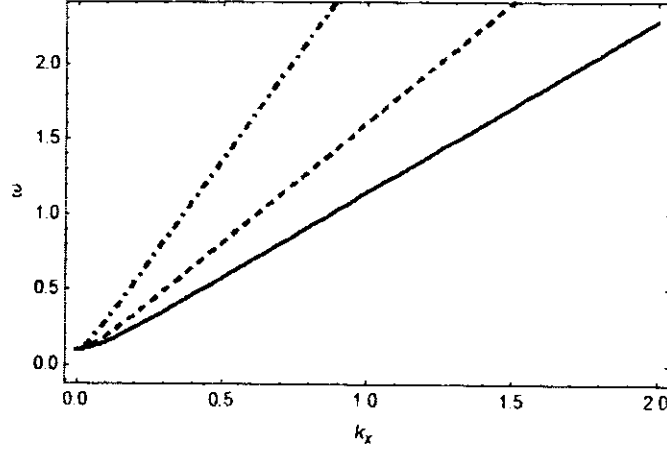


Figure 3.1: Plot of (normalized) frequency ω with respect to (normalized) wavenumber k_x of Eq.(3.13) for different values of plasma number density such that (i) $n_0 \approx 6.38 \times 10^{33} \text{ (m}^{-3}\text{)}$ (Bold, Black) with $g_Q = 0.0345$, $T_F \approx 1.4 \times 10^8 \text{ (}^\circ\text{K)}$, $H \approx 0.00049$, $\varepsilon_0 \approx 0.00046$. (ii) $n_0 \approx 1.78 \times 10^{34} \text{ (m}^{-3}\text{)}$ (Dashed, Red) with $g_Q = 0.0245$, $T_F \approx 2.86 \times 10^8 \text{ (}^\circ\text{K)}$, $H \approx 0.00059$, $\varepsilon_0 \approx 0.00023$. (iii) $n_0 \approx 8.59 \times 10^{34} \text{ (m}^{-3}\text{)}$ (DotDashed, Blue) with $g_Q = 0.0145$, $T_F \approx 8.18 \times 10^8 \text{ (}^\circ\text{K)}$, $H \approx 0.00076$, $\varepsilon_0 \approx 0.000081$. Other parameters are $l_z = 0.99$, $B_0 = 10^5 \text{ (Tesla)}$.

ω to wavenumber k_x by changing the value of plasma number density with a fixed value of B_0 . Note that both the frequency ω and wavenumber k_x are normalized such that $\omega = \omega/v_A k_0$, $k_x = k_x/k_0$, here k_0 represents reference wave number. It can be observed from Figure (3.1) that the value of frequency is enhancing with the increase value of plasma number density.

On the other hand, Figure 3.2 shows the plot between frequency ω and wavenumber k_x by changing the value of magnetic field strength B_0 with a fixed value of plasma number density n_0 . Again note that the frequency ω as well as wavenumber k_x are normalized such that $\omega = \omega/v_A k_0$, $k_x = k_x/k_0$, here k_0 represents reference wavenumber. It is found from Figure (2.2) that the value of frequency reduces by enhancing the value of magnetic field strength B_0 (i.e. spin magnetization ε_0). It is observed that both the Figure (3.1), i.e. $H > \varepsilon_0$ and Figure (3.2), i.e. $H < \varepsilon_0$ are having opposite trends and behavior to each other. The plots are shown in Figure (3.1) and Figure (3.2) are identical in trend and nomenclature with the plots reported in Ref. [].

The effects on Sagdeev potential curve and solitary structure by changing the values of magnetic field strength B_0 for studying KAWs in dense quantum plasma are shown in Figures (3.3-3.4). We have used typical astrophysical plasma parameters such as B_0

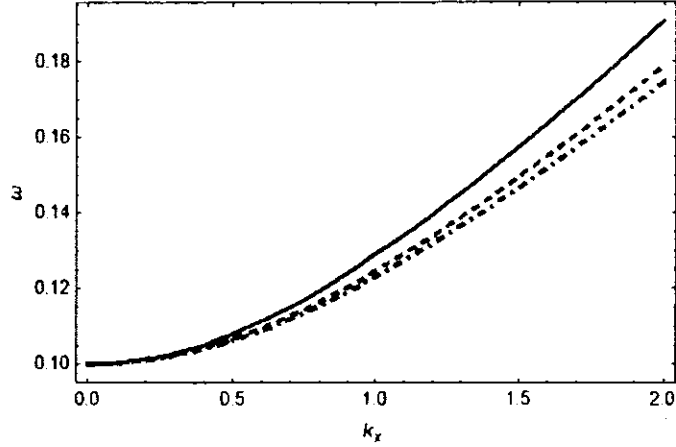


Figure 3.2: Plot of (normalized) frequency ω with respect to (normalized) wavenumber k_x of Eq.(3.13) for different values of magnetic field strength (i.e. spin magnetization energy) such that (i) $B_0 = 2 \cdot 0 \times 10^8(\text{Tesla})$ (Bold, Black) with $\varepsilon_0 \approx 1.54$. (ii) $B_0 = 3 \cdot 0 \times 10^8(\text{Tesla})$ (Dashed, Red) with $\varepsilon_0 \approx 2.30$. (iii) $B_0 = 4 \cdot 0 \times 10^8(\text{Tesla})$ (DotDashed, Blue) with $\varepsilon_0 \approx 3.08$. Other parameters are $T_F \approx 8.68 \times 10^7(^{\circ}K)$, $l_z = 0.99$, $g_Q = 0.0445$, $n_0 \approx 3 \cdot 0 \times 10^{33}(m^{-3})$ and $H \approx 0.00044$.

($\sim 10^7 - 10^8$) *Tesla*, $n_0 \approx 10^{32} m^{-3}$, $T_F \approx 10^7 K$, and ε_0 ($\sim 1.2 - 4.0$). The profiles of Sagdeev potential K for different values of magnetic field strength B_0 from Eq.(3.18) are shown in Figure (3.3). It is found from Figure (3.3) that by increasing the value of parameter B_0 , the depth (width) of Sagdeev potential curves is decreasing while the crossing point (i.e. amplitude) is also increasing in Figure (2.3). The corresponding soliton structure of Figure (3.3) is shown in Figure (3.4) from Eq.(3.20) for different values of magnetic field strength B_0 . It is evident from Figure (3.4) that the both width and amplitude of soliton is increasing by enhancing the value of parameter B_0 . It can be observed from Figure (3.3) that the Sagdeev potential curve gives hump soliton in the sub-Alfvénic region under condition $1 < n < n_m$. This kind of soliton in the sub-Alfvénic region is reported in most of the literature [15].

From graphical analysis, it is revealed that the Sagdeev potential plot is only possible in the sub-Alfvén region if we consider the value of l_z greater than unity such that $l_z^2 > 1$. It's mean that the solitary wave can not exist in the super Alfvénic region when the value of l_z is less than unity such as $l_z^2 < 1$. So, it is very much clear from Figures (3.3-3.4) that we have only one kind of soliton solution and the KAWs can only form hump soliton in the sub-Alfvénic region for value $l_z^2 > 1$. It is also found from our

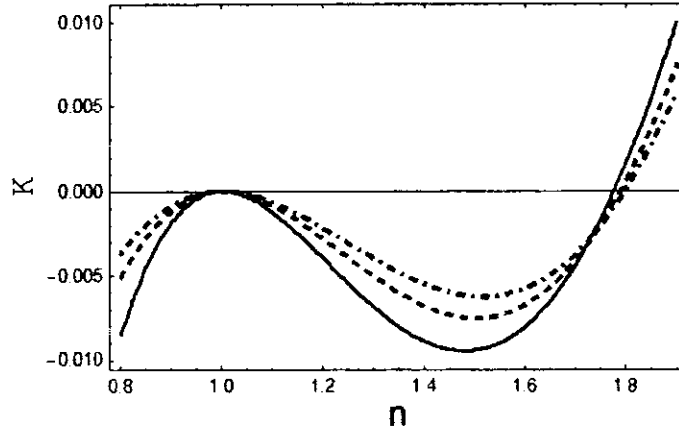


Figure 3.3: Profile of Sagdeev potential curves $K(n)$ against number density n using Eq.(3.18) for different values of magnetic field strength such that (i) $B_0 = 3 \cdot 0 \times 10^7$ (Tesla) (Bold, Black) with $\varepsilon_0 \approx 1.17$. (ii) $B_0 = 6 \cdot 0 \times 10^7$ (Tesla) (Dashed, Red) with $\varepsilon_0 \approx 2.33$. (iii) $B_0 = 9 \cdot 0 \times 10^7$ (Tesla) (DotDashed, Blue) with $\varepsilon_0 \approx 3.50$. Other parameters are $n_0 \approx 2.62 \times 10^{32} (m^{-3})$, $T_F \approx 1.72 \times 10^7 (^\circ K)$, $l_z = \sqrt{1.5}$ and $g_Q = 0.1$.

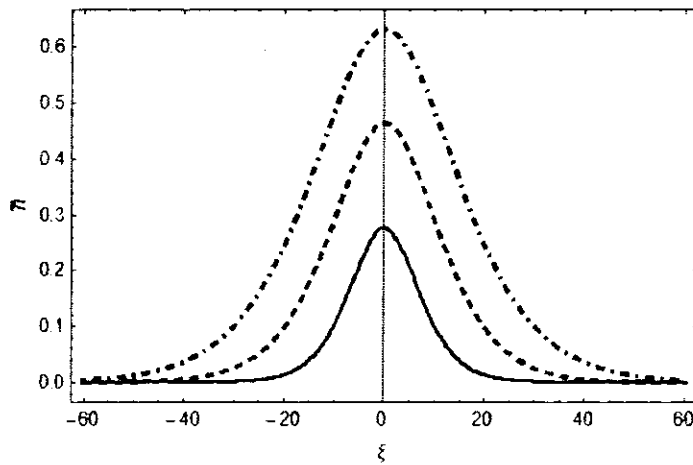


Figure 3.4: Variation of the corresponding solitary wave profiles $\bar{n}(\xi)$ of Figure 3.3 using Eq.(3.20) for different values of spin magnetization energy. All parameters are same as in Figure 3.3.

numerical analysis that the variation found for Sagdeev potential and soliton structure is prominent for parameter B_0 . Furthermore, If we ignore the quantum effects, i.e. Fermi pressure and spin magnetization then the result will be similar as reported in Ref.[17] which is purely for classical plasma case.

3.4 Conclusion

We have investigated the nonlinear propagation characteristics of kinetic Alfvén waves in low- β quantum plasmas by taking into account spin magnetization effects. The Sagdeev potential was derived by using two potential approximation. It is found that kinetic Alfvén hump solitons exist in the presence of spin magnetization effects in the sub-Alfvénic region for value $l_z^2 > 1$. Furthermore, the kinetic Alfvén hump soliton moves with sub-Alfvénic wave speed. It is observed that the changes in linear dispersion relation, Sagdeev potential curves, and soliton structures are significant in the presence of spin magnetization effects. Moreover, If we neglect the quantum effects such as spin magnetization effects then the result will be similar as reported in Ref.[17] for electron classical plasma. Our results may be useful in studying the internal structure of astrophysical compact objects like, white dwarfs, magnetars and pulsars.

Chapter 4

Inertial Alfvén waves in quantum plasma with correction of temperature degeneracy

4.1 Introduction

The Alfvén waves are found to be the main source of heating of the solar and stellar coronae as well as a supplementary heating scheme for fusion plasma devices both theoretically and experimentally. The dispersion relation of shear Alfvén waves in uniform plasma is modified greatly due to large perpendicular wavenumber. So, in other words, when the wavelength perpendicular to background magnetic field is short or wavevector is almost perpendicular to the magnetic field and the phase front is parallel to the field, we have different dispersion relations to shear Alfvén dispersion relation. It is revealed from the data taken by Freja spacecraft that the auroral low-frequency turbulence exhibits strong electromagnetic spikes. From these electromagnetic spikes, the existence of solitary waves with strong density perturbations is observed which reasonably well interpreted as solitary KAWs and IAWs. The observation by Freja satellite showed KAWs and IAWs with density depression and hump type structures [1, 2, 3]. KAWs and IAWs become solitary kinetic Alfvén waves when dispersion canceled out with nonlinearity. Many researchers in the past have studied about solitary KAWs and

IAWs in the classical regime[1, 2, 3, 4, 5].

Alfvén waves attained dispersive nature when electron pressure effects (i.e. $\alpha = \beta/2Q \gg 1$) or electron inertial effects (i.e. $\alpha \ll 1$) in low- β ($= \frac{8\pi n_0 T}{B_0^2}$) plasma are taken into account, where β and Q are the ratio of thermal pressure to magnetic pressure and the ratio of electron mass, to ion mass, respectively. The limiting case $\alpha \gg 1$ gives kinetic Alfvén waves (KAWs), whereas $\alpha \ll 1$ provides inertial Alfvén waves (IAWs). In 1976, Hasegawa and Mima [6] studied the KAWs in low- β plasma (i.e. $\alpha \gg 1$) and found density hump soliton which propagates with the sub-Alfvénic speed in almost parallel to the background magnetic field. Similarly, Shukla et al.[7] have investigated the electron inertial effects on shear Alfvén wave and found dip IAWs solitons with super-Alfvénic speed (i.e. $\alpha \ll 1$).

Quantum plasma has attracted a great deal of interest due to its application in semi-conductors devices[8], nano-structures materials[9], ultra-small electronic devices[10] and in ultra-cold plasmas[11]. Quantum effects are also important in laser-induced plasmas[12] and in astrophysical compact objects like neutron stars, pulsars, magnetars and interior of white dwarf[13]. When the distance among the particle becomes equal to de-Broglie wavelength and pressure degeneracy become equal to classical thermal pressure, then the electron tunneling effects become important in dense plasmas. At high density, due to Pauli exclusion principle, particles follow the Fermi-Dirac distribution function[14, 15, 16, 17]. For degenerate plasmas, the equation of state for both non-relativistic and ultra-relativistic was derived by Chandrasekhar [18]. For the case of degenerate electrons, the equation of state is $p_e \propto n_e^{5/3}$ in non-relativistic limit and for ultra-relativistic case, the equation of state is $p_e \propto n_e^{4/3}$, with p_e, n_e are being the degenerate pressure and degenerate electron density respectively. It is well known that the electrons due to their lower mass are responsible for quantum effects as compared to heavy mass ions and follow Fermi-Dirac statistics and the equation of state is obtained from Fermi-Dirac distribution[19, 20]. By using Fermi-Dirac distribution in terms of polylogarithmic function, Melrose et al.,[21, 22] have investigated the degeneracy effects in quantum plasma in addition to quantum recoil effects. They have obtained the longitudinal response function for various sets of electrostatic waves.

Maxwell-Boltzmann distribution function will be replaced by a Fermi-Dirac distribution function when we consider temperature degeneracy. The parameter $\zeta = \exp\left[\frac{\mu}{k_B T_e}\right]$ in FD describes the degeneracy, is defined in terms of the chemical potential, μ_e with T_e being the electron thermal temperature while k_B is the Boltzmann constant. In non-degenerate limit, $\frac{\mu}{k_B T_e}$ is large and negative, implying $\zeta \rightarrow 0$. When completely degenerate limit approached, $\frac{\mu}{k_B T_e}$ becomes large and positive, implying $\zeta \rightarrow \infty$, with $\mu_e \rightarrow T_F = \frac{1}{2} m_e v_F^2$, where T_F is the Fermi temperature and v_F is the Fermi speed [1, 2]. By employing a similar approach of Refs. [3, 4], the propagation characteristics of ion-acoustic waves were investigated for non-relativistic, unmagnetized and magnetized quantum plasma with electrons degeneracy using the fluid model. They further modified the equation of state by deriving the pressure tensor using the Fermi-Dirac statistics [5, 6].

A magnetohydrodynamic model for a quantum magnetoplasma has been derived by Haas [7]. The dynamics of quantum plasma have been studied extensively from these derived equations [8, 9]. By using the quantum magnetohydrodynamic(QMHD) model [10], the tunneling phenomena and negative differential resistance in semiconductor physics can be elaborated. Recently, the phenomena of collective effects in quantum plasma has gained the attention of many researchers[11, 12, 13, 14, 15, 16, 17]. Using QMHD model, many researchers have studied the quantum effects on propagation characteristics of electrostatic and electromagnetic waves[18, 19, 20, 21, 22, 23, 24]. In MHD theory, it is well known that when the perpendicular wavelength to the external magnetic field becomes comparable to ion larmor radius, The ions don't follow the magnetic field lines due their heavy mass, whereas the electrons still move along the magnetic field lines due to their small larmor radius. Therefore, charge separation is created due to the small difference of the transverse velocities between ions and electrons [25, 26, 27, 28].

We, in this chapter, are discussing the arbitrary temperature degeneracy effect on propagation characteristics of IAWs in intermediate β (i.e. $\alpha \ll 1$ to $\alpha < 1$) quantum plasma. The Korteweg- de Vries equation is derived for studying small-amplitude IAWs by using the reductive perturbation technique in magnetized quantum plasma. The

set of nonlinear equations with derivation is presented in Section 2. Numerical analysis and discussion are presented in Section 3. The summary is then given in the final section.

4.2 Basic Equations

Let's consider a collisionless, homogenous and non-relativistic electron-ion quantum plasma placed in a uniform magnetic field $B = B_0 \hat{z}$ and suppose that the wave is traveling in the $x - z$ plane. To study IAWs in intermediate β (i.e. $\alpha \ll 1$ to $\alpha < 1$) dense plasma, ions are assumed to be classical and inertial, whereas the electrons are taken to be degenerate and inertial. The governing equations to study IAWs in dense plasma with temperature degeneracy correction are given below.

$$\frac{\partial n_e}{\partial t} + \frac{\partial}{\partial z} (n_e v_{ez}) = 0 \quad (4.1)$$

$$\frac{\partial v_{ez}}{\partial t} + v_{ez} \frac{\partial v_{ez}}{\partial z} = -\frac{e}{m_e} E_z - G \left(\frac{k_B T_e}{m_e} \right) \left(\frac{1}{n_e} \frac{\partial n_e}{\partial z} \right) + \frac{\hbar^2}{6m_e^2} \frac{\partial}{\partial z} \left(\frac{\partial^2 \sqrt{n_e}}{\partial z^2} \sqrt{n_e} \right) \quad (4.2)$$

$$\frac{\partial n_i}{\partial t} + \frac{c}{B_0 \Omega_i} \frac{\partial}{\partial x} \left(n_i \frac{\partial E_x}{\partial t} \right) = 0 \quad (4.3)$$

$$\frac{\partial E_x}{\partial z} - \frac{\partial E_z}{\partial x} = -\frac{1}{c} \frac{\partial B_y}{\partial t} \quad (4.4)$$

$$\frac{\partial B_y}{\partial x} = -\frac{4\pi}{c} e n_e v_{ez}, \quad (4.5)$$

here $n_e(n_i)$, v_{ez} , B_0 , and E_x (E_z) are the electron (ion) number density, electron parallel velocity to the uniform external magnetic field and the transverse(longitudinal) electric field respectively. Also, the parameter G is called the degeneracy parameter written in term of polylogarithmic functions such that $G = \frac{Li_{\frac{3}{2}}(-e^{\nu/k_B T_e})}{Li_{\frac{1}{2}}(-e^{\nu/k_B T_e})}$ (i.e. here ν represent the chemical potential with, k_B Boltzmann constant and T_e is the thermal

temperature respectively.

Here Ω_i ($= \frac{eB_0}{cm_i}$), B_y are the the ion cyclotron frequency, the sheared magnetic field and c being the light speed. Noting that in the current study, the ion inertia, ion current density, and displacement current have been ignored. Additionally, only electrons possess quantum effects as compared to large mass ions.

For nearly non-degenerate (NND) (G_{NND}) limit $\xi \ll 1$, we expand the polylogarithmic function as $Li_x(-\xi) = -\xi + \frac{(-\xi)^2}{2x}$ which makes the $G_{NND} = (1 + \frac{\xi}{2})$. For complete non-degenerate plasma (i.e. $\xi \rightarrow 0$) which gives $G_{NND} = 1$. Whereas, for nearly degenerate (ND) limit (G_{ND}) $\xi \gg 1$, the polylogarithmic function can be expanded as $-Li_x(-\xi) = \frac{(\ln \xi)^x}{\Gamma(x+1)}$. Using then the Sommerfeld lemma [15, 16] $v = k_B T_F \left[1 - \frac{\pi^2}{12} \left(\frac{T_e}{T_F} \right)^2 \right]$ and hence $\ln \xi = \frac{T_F}{T_e} - \frac{\pi^2}{12} \frac{T_e}{T_F}$ that implies $G_{ND} = \frac{2}{3} \frac{1}{\delta} \left(1 - \frac{\pi^2}{12} (\delta)^2 \right)$. For complete degenerate limit (i.e. $\delta \left(= \frac{T_e}{T_F} \right) \rightarrow 0$), $v \rightarrow T_F = \frac{1}{2} m_e v_F^2$ with T_F and v_F being the Fermi temperature and Fermi speed, respectively.

Now we study the effect of temperature degeneracy on linear properties of inertial Alfvén waves in dense plasma. We have dispersion relation as $\omega^2 = \frac{v_A^2 k_x^2}{1 + k_x^2 \lambda_e^2} \left(1 + k_x^2 G \frac{k_B T_e}{\Omega_i^2} \right)$ using Eqs.(4.1) to (4.5), where $v_A = \left(\frac{B_0^2}{4\pi n_0 m_i} \right)^{\frac{1}{2}}$, $\lambda_e = \frac{c}{\omega_{pe}}$, $\omega_{pe} = \left(\frac{4\pi n_0 e^2}{m_e} \right)^{\frac{1}{2}}$ and k denote the Alfvén speed, electron inertial length, electron plasma frequency and wave number respectively. Noting that the presence of temperature degeneracy significantly affects ion gyro-radius. If we ignore the effects of temperature degeneracy, we obtained the same result for dispersion relation as reported by Ref.[17] in case of pure classical plasma

Now, we use dimensionless parameters as $\bar{n} = \frac{n}{n_0}$, $\bar{t} = \Omega_i t$, $\bar{v} = \frac{v}{v_A}$, $\bar{x} = \frac{x}{\lambda_e}$, $\bar{z} = \frac{z \Omega_i}{v_A}$, $\bar{E}_x = \frac{E_x}{B_0}$, $\gamma = \left(\frac{m_i}{m_e} \right)^{\frac{1}{2}} \frac{c}{v_A}$, $\Omega_i = \frac{e B_0}{c m_i}$. So, Eqs.(4.1) to (4.5) are given below,

$$\frac{\partial n}{\partial \bar{t} / \Omega_i} \times \bar{n} n_0 + \frac{\partial}{\partial \bar{z}} \times \frac{v_A}{\Omega_i} \times \bar{n} n_0 \times \bar{v} v_A = 0, \quad (4.6)$$

$$n_0 \Omega_i \frac{\partial n}{\partial \bar{t}} + n_0 v_A \times \frac{\Omega_i}{v_A} \frac{\partial}{\partial \bar{z}} n v = 0, \quad (4.7)$$

$$\frac{\partial n}{\partial t} + \frac{\partial}{\partial z} n v = 0, \quad (4.8)$$

and

$$\frac{\partial}{\partial \bar{t}/\Omega_i} \bar{n} n_0 + \frac{c}{B_0 \Omega_i} \times \frac{\partial n}{\partial \bar{x} \lambda} \times \bar{n} n_0 \times \frac{\partial}{\partial \bar{t}/\Omega_i} E_x B_0 = 0, \quad (4.9)$$

$$n_0 \Omega_i \frac{\partial}{\partial \bar{t}} \bar{n} + \frac{c}{B_0 \Omega_i} \times \frac{\omega_{pe}}{c} \times n_0 B_0 \Omega_i \times \frac{\partial}{\partial \bar{x}} (\bar{n} \frac{\partial}{\partial \bar{t}} E_x) = 0, \quad (4.10)$$

$$\Omega_i \frac{\partial}{\partial \bar{t}} \bar{n} + \omega_{pe} \frac{\partial}{\partial \bar{x}} (\bar{n} \frac{\partial}{\partial \bar{t}} E_x) = 0, \quad (4.11)$$

$$\frac{\partial}{\partial \bar{t}} \bar{n} + \frac{\omega_{pe}}{\Omega_i} \frac{\partial}{\partial \bar{x}} (\bar{n} \frac{\partial}{\partial \bar{t}} E_x) = 0, \quad (4.12)$$

$$\frac{\partial n}{\partial t} + \gamma \frac{\partial}{\partial x} \left(n \frac{\partial E_x}{\partial t} \right) = 0, \quad (4.13)$$

where $\gamma = \frac{\omega_{pe}}{\Omega_i} = \frac{c}{v_A} \left(\frac{m_i}{m_e} \right)^{\frac{1}{2}}$.

and

$$\frac{\partial}{\partial \bar{x} \times \frac{v_A}{\Omega_i}} \times E_x B_0 - \frac{\partial}{\partial x \times \frac{c}{\omega_{pe}}} E_z B_0 = -\frac{1}{c} \times \frac{\partial}{\partial \bar{t}/\Omega_i} B_y, \quad (4.14)$$

$$\frac{\Omega_i B_0}{v_A} \frac{\partial E_x}{\partial \bar{x}} - \frac{\omega_{pe} B_0}{c} \frac{\partial E_z}{\partial x} = -\frac{\Omega_i}{c} \times \frac{\partial B_y}{\partial \bar{t}}, \quad (4.15)$$

$$\frac{B_0 \Omega_i}{v_A} \frac{\partial E_x}{\partial z} - \frac{B_0 \omega_{pe}}{c} \frac{\partial E_z}{\partial x} = \frac{-\Omega_i}{c} \frac{\partial B_y}{\partial \bar{t}}, \quad (4.16)$$

$$\frac{\partial v}{\partial t} + v \frac{\partial v}{\partial z} = -\gamma \left(\frac{m_i}{m_e} \right)^{\frac{1}{2}} E_z - G \frac{k_B T_e}{m_e v_{A^2}} \left(\frac{1}{n} \frac{\partial n}{\partial z} \right) + \frac{H^2}{2} \frac{\partial}{\partial z} \left(\frac{\frac{\partial^2}{\partial z^2} \sqrt{n_e}}{\sqrt{n_e}} \right), \quad (4.17)$$

and

$$\frac{\partial}{\partial \bar{x} \times \frac{c}{\omega_{pe}}} \times B_y = \frac{-4\pi}{c} e n n_0 v v_A \quad (4.18)$$

$$\frac{\partial B_y}{\partial x} = \frac{-4\pi}{c} \times ev_A \times nn_0v \times \frac{c}{\omega_{pe}} \quad (4.19)$$

$$\frac{\partial B_y}{\partial x} = \frac{-4\pi en_0v_A}{\omega_{pe}} (nv). \quad (4.20)$$

Here, $H = \frac{\Omega_i}{\sqrt{3m_e v_A^2}}$ has been used as dimensionless parameter which is the result of quantum diffraction effect. Now, we use the stretched variables as follow:

$$\eta = \epsilon(z - t), \quad \zeta = \epsilon^{\frac{1}{2}}x, \quad \tau = \epsilon^2t, \quad (4.21)$$

and the perturbed quantities can be expanded around equilibrium as follow:

$$n = 1 + \epsilon n^{(1)} + \epsilon^2 n^{(2)} + \dots \quad (4.22)$$

$$v = \epsilon v^{(1)} + \epsilon^2 v^{(2)} + \dots \quad (4.23)$$

$$\gamma E = 1 + \epsilon E^{(1)} + \epsilon^2 E^{(2)} + \dots, \quad (4.24)$$

where parameter $\epsilon \ll 1$ represents the amplitude of the perturbation. Substituting Eqs. (4.21) to (4.24) into Eqs.(4.8) to (4.20) and collecting the terms of lowest order of ϵ , we obtain

$$n^{(1)} = v^{(1)} = -\frac{\partial E^{(1)}}{\partial \zeta} \quad (4.25)$$

To next orders (i.e. ϵ^2), we have

$$\frac{\partial n^{(1)}}{\partial \tau} - \frac{\partial}{\partial \eta} \left(n^{(2)} + \frac{\partial E^{(2)}}{\partial \zeta} \right) - \frac{\partial}{\partial \zeta} \left(n^{(1)} \frac{\partial E^{(1)}}{\partial \eta} \right) + \frac{\partial}{\partial \zeta} \frac{\partial E^{(1)}}{\partial \tau} = 0, \quad (4.26)$$

and

$$-2\frac{\partial n^{(1)}}{\partial \tau} + \frac{\partial}{\partial \eta} \left(n^{(2)} + \frac{\partial E^{(2)}}{\partial \zeta} \right) - \left(1 - G \frac{k_B T_e}{m_e v_A^2} \right) \frac{\partial^2}{\partial \zeta^2} \frac{\partial n^{(1)}}{\partial \eta} = 0. \quad (4.27)$$

Noting that the dimensionless parameter $H = \frac{\hbar \Omega_i}{\sqrt{3m_e v_A^2}}$ which is showing the behavior of quantum diffraction will be ignored when considering the higher order terms (i.e. ϵ^3 and ϵ^4) in Eq.(4.27). Combining Eqs.(4.26) and (4.27), we have

$$2\frac{\partial n^{(1)}}{\partial \tau} - n^{(1)} \frac{\partial n^{(1)}}{\partial \eta} + \frac{\partial n^{(1)}}{\partial \zeta} \frac{\partial E^{(1)}}{\partial \eta} + \left(1 - G \frac{k_B T_e}{m_e v_A^2} \right) \frac{\partial^2}{\partial \zeta^2} \frac{\partial n^{(1)}}{\partial \eta} = 0 \quad (4.28)$$

Both Eqs. (4.28) and (4.25) give the evolution of the stationary wave solution. Using planar coordinate $\mu = K_x \zeta + K_z \eta - \Delta \tau$, we can verify the stationary traveling wave solution of Eq.(4.28) as

$$\delta n = -A_m \sec h^2[W\mu], \quad (4.29)$$

here $A_m = 3 \left(\frac{M-1}{K_x} \right)$ and $W = \sqrt{\frac{M-1}{\left(1 - G \frac{k_B T_e}{m_e v_A^2} \right) K_x^2 K_z}}$ represent the peak amplitude and width of localized pulse respectively. This is generalized soliton solution of IAWs with arbitrary temperature degeneracy.

Noting that the width of the solitary inertial Alfvén wave will be changed substantially in the presence of arbitrary temperature degeneracy. If we ignore the effects of temperature degeneracy in Eq.(4.29), we obtained same result as reported by Ref.[] for $\alpha \ll 1$. For NND limiting case such as $\xi \ll 1$, we obtained the following relation from Eq.(4.29).

$$W = \sqrt{(M-1) / \left(1 - \left(1 + \frac{\xi}{2^{\frac{3}{2}}} \right) \left(\frac{k_B T_e}{m_e v_A^2} \right) \right) K_x^2 K_z}. \quad (4.30)$$

When the parameter ξ approaches to zero (i.e. $\xi \rightarrow 0$) which means complete NND plasma limiting case, we obtained

$$W = \sqrt{(M-1) / \left(1 - \left(\frac{k_B T_e}{m_e v_A^2}\right)\right)} K_x^2 K_z. \quad (4.31)$$

In similar way, for ND limiting case such as $\xi \gg 1$, we obtained

$$W = \sqrt{(M-1) / \left(1 - \frac{2 k_B T_F}{3 m_e v_A^2} \left(1 - \frac{\pi^2}{12} (\delta)^2\right)\right)} K_x^2 K_z. \quad (4.32)$$

When the parameter δ approaches to zero (i.e. $\delta \rightarrow 0$) which means complete ND, we obtained

$$W = \sqrt{(M-1) / \left(1 - \frac{2 k_B T_F}{3 m_e v_A^2}\right)} K_x^2 K_z. \quad (4.33)$$

4.3 Numerical Analysis and Discussion

Astrophysical plasmas existing in astrophysical compact stars such as white dwarfs, pulsars, and magnetars are characterized by strong magnetic fields $B \approx (10^{11} - 10^{15}) G$, whereas the plasma number densities are thought to have $n_0 \approx (10^{25} - 10^{29}) cm^{-3}$ [1, 2, 3]. Usually, we use general coupling parameter Λ to describe the collisional or collisionless state of quantum plasma having arbitrary temperature degeneracy. The general coupling parameter can be defined as the ratio of the interaction energy to the Fermi energy. Noting that for higher values of plasma densities, the collective effects dominate in quantum plasma (i.e. when the quantum coupling parameter is small, we have quantum collisionless regime). The expression for general coupling parameter is $\Lambda = 1/6 (4/3\pi^2)^{1/3} e^2 n_0^{1/3} / \epsilon_0 k_B T_e \times Li_{3/2}(-\xi) / Li_{1/2}(-\xi)$. The plasma number density and thermal(Fermi) temperature play a crucial role in studying IAWs in collisionless intermediate β (i.e. $\alpha \ll 1$ to $\alpha < 1$) dense quantum plasma for both NND and ND plasma limiting case. For this purpose, we use the general coupling parameter Λ to calculate the value of plasma number density and thermal(Fermi) temperature. In this section, we will discuss the numerical plots to study inertial Alfvén solitons using Eq.(4.29) for NND and ND plasma limits. Here, we have used values of different parameters in CGS system such as plasma number density $n_0 \approx (2.3 \times 10^{24}$ to

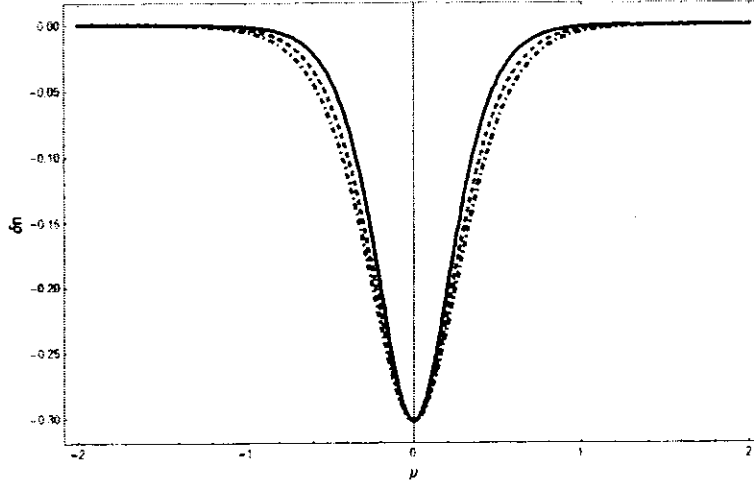


Figure 4.1: The dip soliton structure (nearly non-degenerate) is plotted between δn and μ for (i) $\xi = 0.92$ (Bold, Black) with $\alpha \approx 0.41$, $n_0 \approx 3.5 \times 10^{24} \text{ cm}^{-3}$ and $T_e \approx 3.7 \times 10^6 \text{ K}$, (ii) $\xi = 0.94$ (Dashed, Red) with $\alpha \approx 0.31$, $n_0 \approx 2.9 \times 10^{24} \text{ cm}^{-3}$ and $T_e \approx 3.4 \times 10^6 \text{ K}$ and (iii) $\xi = 0.96$ (DotDashed, Blue) with $\alpha \approx 0.21$, $n_0 \approx 2.3 \times 10^{24} \text{ cm}^{-3}$ and $T_e \approx 3.1 \times 10^6 \text{ K}$. Other parameters are, $B_0 = 10^{10} \text{ G}$, $K_x = 0.1$, $M = 1.1$ and $\Lambda = 0.0005$.

$1.8 \times 10^{27} \text{ cm}^{-3}$, general coupling parameter $\Lambda = (0.0005 \text{ to } 0.001)$, thermal temperature $T_e \approx (1.04 \times 10^6 \text{ to } 3.7 \times 10^6) \text{ K}$, Fermi temperature $T_F \approx (2.7 \times 10^7 \text{ to } 7.1 \times 10^7) \text{ K}$ and magnetic field $B_0 = (10^9 - 10^{12}) \text{ G}$. Figure 4.1 shows the solitary wave structure with density depression for the NND plasma limiting case. Here, we have used parameters like $\xi (= 0.92, 0.94, 0.96)$, $\alpha \approx (0.41, 0.31, 0.21) < 1$, $B_0 = 10^{10} \text{ G}$, $T_e = (3.1 \times 10^6 - 3.7 \times 10^6 \text{ K})$, $n_0 = (2.3 \times 10^{24} - 3.5 \times 10^{24} \text{ cm}^{-3})$, $M = 1.1$ and $\Lambda = 0.0005$. It is found from Figure (4.1) that the width of dip solitons is broadening by enhancing the value of parameter ξ , whereas no change observed in amplitude.

Figure 4.2 shows a solitary wave structure with density depression for the ND plasma limiting case. Here, we have used parameters like $n_0 = (4.1 \times 10^{26} \text{ to } 1.8 \times 10^{27} \text{ cm}^{-3})$, $T_e = (2.7 \times 10^7 \text{ to } 7.1 \times 10^7 \text{ K})$, $\delta (= 0.65, 0.75, 0.85)$, $\alpha \approx (0.06, 0.26, 0.86) < 1$, $B_0 = 10^{11.8} \text{ G}$, $M = 1.1$ and $\Lambda = 0.001$. It is clear from Figure (4.2) that the width of dip soliton is decreasing by enhancing the value of parameter δ , whereas no change observed in amplitude.

On the other hand, Figure (4.3) shows hump solitary wave structure for NND plasma limiting case. Here, we have used parameters like $\xi (= 0.88, 0.89, 0.90)$, $\alpha \approx (0.99, 0.88, 0.77) < 1$, $B_0 = 10^{9.2} \text{ G}$, $T_e = (1.01 \times 10^6 - 1.11 \times 10^6 \text{ K})$, $n_0 =$

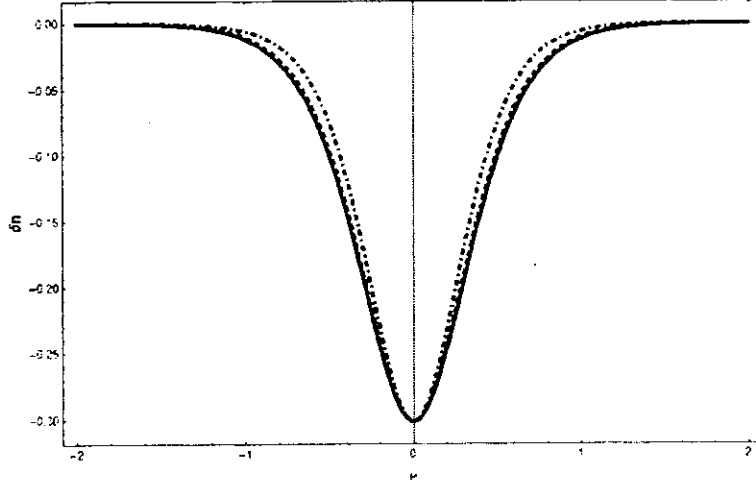


Figure 4.2: The dip soliton profile (nearly degenerate) of δn versus μ for $\delta = 0.65$ (Bold, Black) with $\alpha \approx 0.06$, $n_o \approx 4.1 \times 10^{26} \text{ cm}^{-3}$ and $T_F \approx 2.7 \times 10^7 \text{ K}$, (ii) $\delta = 0.75$ (Dashed, Red) with $\alpha \approx 0.26$, $n_o \approx 8.0 \times 10^{26} \text{ cm}^{-3}$ and $T_F \approx 4.1 \times 10^7 \text{ K}$, and (iii) $\delta = 0.85$ (DotDashed, Blue) with $\alpha \approx 0.86$, $n_o \approx 1.8 \times 10^{27} \text{ cm}^{-3}$ and $T_F \approx 7.1 \times 10^7 \text{ K}$. Other parameters are, $B_0 = 10^{11.8} \text{ G}$, $K_x = 0.1$, $M = 1.1$ and $\Lambda = 0.001$.

($5.9 \times 10^{23} - 7.05 \times 10^{23} \text{ cm}^{-3}$), $M = 0.9$ and $\Lambda = 0.00097$. It is clear from Figure (4.3) that the width of hump soliton is decreasing by enhancing the value of parameter ξ , while no change observed in amplitude.

Note that we obtained IAWs hump soliton by considering thermal pressure for the NND case with $\alpha < 1$, which can not be found without thermal pressure effects. We can obtain the result of Ref.[] for purely plasma case with $\alpha \ll 1$, when the quantum effects are ignored such that degenerate pressure correction term approaches to zero (i.e. $T_e \rightarrow 0$)

4.4 Conclusion

We have investigated the nonlinear propagation characteristics of inertial Alfvén waves in intermediate β (i.e. $\alpha \ll 1$ to $\alpha < 1$) quantum plasmas by taking into account arbitrary temperature effects in term of NND and ND plasma limiting case. By employing a reductive perturbation, Korteweg- de Vries (KdV) equation was derived for a small amplitude limit. It is found that in the presence of thermal temperature both IAWs dip and hump solitons exist in NND and ND plasma limiting case. It is observed

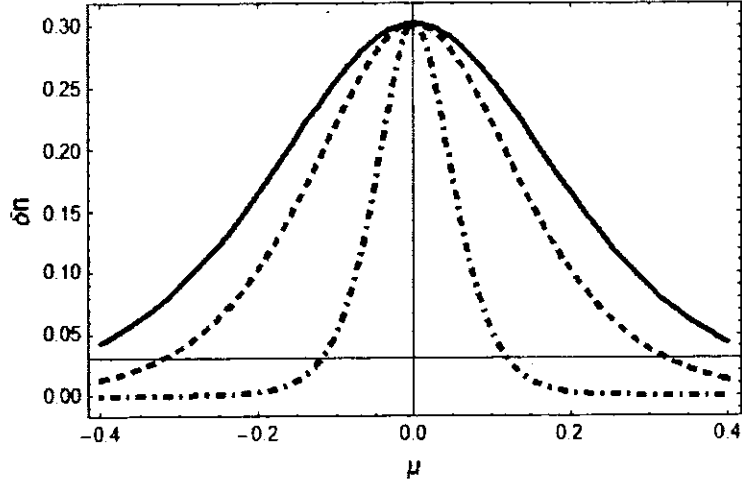


Figure 4.3: The hump soliton structure (nearly non-degenerate) is plotted between δn and μ for (i) $\xi = 0.88$ (Bold, Black) with $\alpha \approx 0.99$, $n_o \approx 7.05 \times 10^{23} \text{cm}^{-3}$ and $T_e \approx 1.1 \times 10^6 \text{K}$, (ii) $\xi = 0.89$ (Dashed, Red) with $\alpha \approx 0.88$, $n_o \approx 6.4 \times 10^{23} \text{cm}^{-3}$ and $T_e \approx 1.07 \times 10^6 \text{K}$, and (iii) $\xi = 0.90$ (DotDashed, Blue) with $\alpha \approx 0.77$, $n_o \approx 5.9 \times 10^{23} \text{cm}^{-3}$ and $T_e \approx 1.04 \times 10^6 \text{K}$. Other parameters are, $B_0 = 10^{9.2} \text{G}$, $K_x = 0.1$, $M = 0.9$ and $\Lambda = 0.00097$.

that the changes in soliton structures for NND and ND plasma state are significant. Moreover, If we neglect the quantum effects such as arbitrary temperature degeneracy effects for both NND and ND plasma limiting case (i.e. $\zeta = \delta = 0$) than the result will be similar as reported in Ref.[] for electron-ion classical plasma. Our results may be useful in studying the structure of astrophysical compact objects like, white dwarfs, magnetars and pulsars.

Chapter 5

The effect of exchange-correlation and spin magnetization on inertial Alfvén waves in dense plasma

5.1 Introduction

Over the past few years, a great deal of interest has been devoted to study the dynamics of quantum plasma in connection to its likely application in nanostructures material(i.e. metallic and semiconductor)[1] as well as in astrophysical objects under extreme condition (i.e. white dwarfs and magnetars)[2]. The high degree of miniaturization in electronic devices is possible due to the presence of quantum mechanical effects in the system [3]. Consequently, the effects due to spin magnetization, Fermi pressure, and exchange-correlation potential would play a crucial role in the construction of electronic devices for future purposes[4, 5, 6, 7]. When the electron density is sufficiently large and the temperature is too low, the exchange-correlation effects in quantum plasma can no longer be ignored and particularly when spin correlation effects are present in the system. The exchange-correlation potential V_{xc} can be described as a function of the electron density[8, 9, 10, 11]. In the past, most of the studies have focused their attention to see the effect of exchange-correlation on electron gas especially in quantum wells[12, 13]. Recently, many researchers have investigated the

effects of exchange-correlation on solitary ion-acoustic waves as well as on parametric instabilities in quantum plasma system [12, 13, 14]. Also, Rimza et al.[15] have discussed the influence of exchange-correlation, degeneracy pressure and Bohm potential on the lower hybrid wave in two-component quantum plasma. The effects of exchange-correlation (along with Bohm potential and spin force) on magnetosonic shocks in a spin-1/2 quantum dissipative plasma was studied by Sahu and Misra.[16]. They have observed that the exchange-correlation effects are more dominant and responsible in the transition from monotonic to oscillatory shocks to other quantum effects.

On the other hand, there has been a great deal of interest in excitations of collective modes in the spin system, such as spin waves. In magnetized plasmas, the electron spin has two eigenstates, namely, spin-up and spin-down relative to the background magnetic field B_0 . In equilibrium plasmas, the average value of spin could be approximated by $S = -\hbar M/2\mu_B n_e$. Therefore, the spin effects are important only in the case of very high ambient magnetic field intensity and very low plasma temperature, and can be neglected in the common plasmas ($\mu_B B_0 \ll k_B T_e$). Nevertheless, the equilibrium will be broken when an electromagnetic (EM) wave with spatial nonuniform intensity entering the plasmas. Due to the spin contribution to the ponderomotive force act in opposite direction for spin-up and spin-down electrons [17], these two kinds of electrons will be separated, at least partly. So, in the local region, the spin no longer canceled each other completely, i.e. a spin-polarized plasma is induced, which in turn modifies the dispersion properties and contributes to the nonlinear interaction of EM wave and plasma. Marklund et al. have studied the characteristics of nonlinear magnetosonic waves in strongly magnetized quantum plasma with quantum Bohm potential and electron spin-1/2 effects[18]. Many researchers have studied the nonlinear waves in quantum plasmas including the quantum statistics, quantum diffraction and spin effects[19, 20, 21, 22, 23, 24, 25].

Alfvén waves are ubiquitous in nature which attained dispersive nature when electron pressure effects (i.e. $\alpha \equiv \beta/2Q \gg 1$) or electron inertial effects (i.e. $\alpha \ll 1$) in low- β plasma are taken into account. The limiting case $\alpha \gg 1$ gives kinetic Alfvén waves (KAWs), whereas $\alpha \ll 1$ provides inertial Alfvén waves (IAWs)[26, 27]. The

data from Freja spacecraft have provided the evidence for the existence of both KAWs and IAWs in aurora and cusp region [17]. It is observed by Cluster and Fast spacecraft that in the presence of the finite parallel electric field, IAWs can accelerate the electrons in polar region of earth magnetosphere and ionosphere[18]. In 1976, Hasegawa and Mima [19] studied the KAWs in low- β plasma (i.e. $\alpha \gg 1$) and found density hump soliton which propagates with the sub-Alfvén speed in almost parallel to the background magnetic field. Later on, by extending the similar studies in inertial limit, Shukla et al.[20] observed IAWs with density dip propagating along the magnetic field with super-Alfvénic speed for $\alpha \ll 1$.

We, in this manuscript, are discussing the electron exchange-correlation and spin magnetization effects on propagation characteristics of IAWs in low- β quantum plasma (i.e. $\alpha \ll 1$). The Sagdeev's potential is derived for studying an arbitrary amplitude IAWs whereas, Korteweg de Vries equation is derived for studying small-amplitude IAWs by using reductive perturbation technique in a magnetized quantum plasma. The set of nonlinear equations with derivation is presented in Section 2. Numerical analysis and discussion are presented in Section 3. The summary is then given in the final section.

5.2 Basic Equations

Consider a collisionless electron-ion quantum plasma placed in a uniform magnetic field B directed along the z -axis with $\alpha \ll 1$. Here, the electrons are considered to be inertial and degenerate having spin and exchange-correlation effects, while, the ions are taken to be dynamic and classical. All the variations take place in the $x - z$ direction. Due to low- β assumption, one can apply two potentials ψ (longitudinal) and ϕ (transverse) related with electric fields such that $E_z = -\partial_z \psi$ and $E_x = -\partial_x \phi$ [21]. The governing equations for studying IAWs in low- β quantum plasmas are given below. Thus according to the geometry of the problem electron continuity, momentum (i.e. electrons move along the magnetic field lines due to their small Larmor radius) and spin evolution equations are, respectively given as:

$$\partial_t n_e + \partial_z (n_e v_{ez}) = 0, \quad (5.1)$$

$$\partial_t v_{ez} + v_{ez} \partial_z v_{ez} = -\frac{e}{m_e} E_z - \frac{1}{m_e n_e} \partial_z P_{Fe} + \frac{2\mu}{m_e \hbar} \partial_z (\mathbf{S} \cdot \mathbf{B}) - \frac{1}{m_e} \partial_z V_{xc}, \quad (5.2)$$

$$(\partial_t + v_e \cdot \nabla) S = \frac{2\mu}{\hbar} (\mathbf{S} \times \mathbf{B}) \quad (5.3)$$

where n_e is the electron number density, v_{ez} is the electron velocity, e is the electron charge, and m_e is the mass. The second term in Eq.(5.2) represents electron Fermi pressure $P_{Fe} (= \frac{m_e v_{Fe}^2}{3n_e^2} n_e^3)$. Here, the Fermi pressure has been added as a correction term and due to low- β assumption, its impact is almost negligible for studying IAWs in magnetized quantum plasmas.

The third term in Eq.(5.2) represents the spin force. Here μ_B represents Bohr magneton (i.e. $\mu_B = \frac{e\hbar}{2m_e}$) and for the lowest order spin analysis, $S = -\frac{\hbar \mathbf{M}}{2\mu_B n_e}$, with magnetization vector $\mathbf{M} = \left(\frac{n_e \mu_B^2}{\epsilon_{Fe}} \right) \mathbf{B}$. The last term of Eq.(5.2) represents the exchange-correlation potential V_{xc} for the electron gas. The adiabatic local-density approximation gives the exchange-correlation term as a function of the electron density [1, 2]. The study of exchange-correlation become important in dense quantum plasmas due to the presence of high electron density and low temperature. Also, due to the rapid development of modern technology (i.e. with great degree of miniaturization of nanostructures electronic devices), the contribution of exchange-correlation effects can no longer be ignored. Additionally, the presence electrons spin effects in the system further enhance the significance of exchange-correlation. Note that the exchange-correlation is strongly dependent on density correlation as well as on spin correlation effects. The exchange correlation term can be expressed as: [3] $V_{xc} = 0.985(e^2/4\pi\epsilon_0)n_e^{\frac{2}{3}}[1 + 0.034/a_B^* n_e^{\frac{1}{3}} \ln(1 + 18.37a_B^* n_e^{\frac{1}{3}})]$. In simple form, it reads as: $V_{xc} = -1.6 \frac{e^2}{4\pi\epsilon_0} n_e^{\frac{1}{3}} + 5.65 \frac{\hbar^2}{m_e} n_e^{\frac{2}{3}}$, when $18.37a_B^* n_e^{\frac{1}{3}} \ll 1$, where $a_B^* = \frac{4\pi\epsilon_0 \hbar^2}{m_e e^2}$. The perpen-

dicular velocities of classical ion are given as:

$$v_{i\perp} = v_E + v_{pi}, \quad (5.4)$$

where $v_E = \frac{\hat{z} \times E_x}{B_0}$ and $v_{pi} = -\frac{1}{B_0 \Omega_i} \left(\partial_t + \frac{(\hat{z} \times \nabla_{\perp} \phi) \cdot \nabla}{B_0} \right) \nabla_{\perp} \phi \hat{x}$ represents the $E \times B$ drift and ion polarization drift respectively and $\Omega_i = \left| \frac{eB_0}{m_i} \right|$ is the ion gyrofrequency with m_i being mass of ion. Since $E \times B$ drift is more influential and in the limit of $|\partial_t| \ll \Omega_i$, with application of E_x gives the ion polarization drift in simplified form as:

$$v_{pi} = \frac{1}{B_0 \Omega_i} \partial_t E_x. \quad (5.5)$$

In order to avoid vector nonlinearity, the nonlinear term $\frac{(\hat{z} \times \nabla_{\perp} \phi) \cdot \nabla}{B_0} \nabla_{\perp} \phi$ of convective derivative can be ignored for weak dispersion. Moreover, we have also neglected the effects of ion parallel motion along the magnetic field due to low- β assumption. Using Eq.(5.5) in ion continuity equation $\partial_t n_i + \partial_x (n_i v_{pi}) = 0$ we have:

$$\partial_t n_i + \frac{1}{B_0 \Omega_i} \partial_x (n_i \partial_t E_x) = 0. \quad (5.6)$$

Faraday's law $\nabla \times E = -\partial_t B$ for the two potential theory can be expressed as:

$$\partial_z E_x - \partial_x E_z = -\partial_t B_y. \quad (5.7)$$

Ampere's law with spin magnetization density M can be written as:

$$\partial_x B_y = \mu_0 J_t, \quad (5.8)$$

where $J_t = J_z + J_M$, with J_z being the polarization current density and $J_M = \nabla \times M$ is the electron spin magnetization current density. The total magnetic field contains both the free (i.e. $J = qnv$) and spin electron contributions. Additionally, in above Eq.(5.8) the displacement current contribution has been ignored because of low frequency perturbation approximation. The quasi-neutrality condition $n_i \simeq n_e \simeq n$ implies that $\nabla \cdot J = 0$ and further depicts:

$$\partial_x J_{ix} = -\partial_z J_t, \quad (5.9)$$

with $J_{ix} = e(n_i v_{pi})$. Thus, electron continuity Eq.(5.1) becomes:

$$\partial_t(en_e) = \partial_z J_t, \quad (5.10)$$

here because of the low- β assumption, the contribution of ions to the current density is negligible; hence J_z is given by the electron density. It is to be noted here that the total parallel current due to electrons (i.e. J_t) is canceled out due to ion polarization current.

The linear dispersion relation of IAWs by using the linearized form of Eqs.(5.1), (5.2), (5.6), (5.7) and (5.8) with plane wave solution can be written as

$$\omega = \frac{v_A k_z}{\sqrt{1 + k_x^2 \lambda_e^2}} \left[1 + k_x^2 \Upsilon \left(\varepsilon_0^2 + \frac{\gamma}{3} - \frac{2\lambda}{3} - 2 \right) \right]^{1/2} \quad (5.11)$$

where $v_A = \left(\frac{B_0^2}{\mu_0 n_0 m_i} \right)^{1/2}$ is the Alfvén velocity, $\lambda_e = \frac{c}{\omega_{pe}}$ represents the electron inertial length, $\omega_{pe} = \left(\frac{n_0 e^2}{\varepsilon_0 m_e} \right)^{1/2}$ is the electron plasma frequency, $k_{x,z}$ represents the wavenumber and $\Upsilon = \frac{E_{Ex}}{m_i \Omega_i^2}$. It is important to mention that the IAWs transports energy slowly in transverse direction for $k_x \gg k_z$ [].

For convenience, we use the rescaling $\bar{n} = \frac{n}{n_0}$, $\bar{t} = \Omega_i t$, $\bar{v}_{ez} = \frac{v_{ez}}{v_A}$, $(\bar{x}, \bar{z}) = (x, z) \frac{\Omega_i}{v_A}$, $\bar{E}_{x,z} = \left(\frac{e v_A}{\Omega_i E_{Fe}} \right) E_{x,z}$ and $\bar{B}_y = \frac{B_y}{B_0}$. Introducing the variables and dropping the bars, Eqs.(5.1), (5.2), (5.6), (5.7) and (5.8) in normalized form are given below:

$$\partial_t n + \partial_z (n v_{ez}) = 0, \quad (5.12)$$

$$\frac{1}{\sigma} (\partial_t v_{ez} + v_{ez} \partial_z v_{ez}) = -E_z - 2n \partial_z n + \varepsilon_0^2 \partial_z \ln n_e + \gamma \partial_z n^{1/3} - \lambda \partial_z n^{2/3}, \quad (5.13)$$

$$\partial_t n + F \partial_x (n \partial_t E_x) = 0, \quad (5.14)$$

$$F (\partial_x \partial_z^2 E_x - \partial_z \partial_x^2 E_x) = -\partial_t^2 n, \quad (5.15)$$

where $\varepsilon_0 = \frac{\mu_B B_0}{E_F}$ describes the normalized Zeeman energy due to the spin magnetization with $\sigma = \frac{v_{Fz}^2}{2v_A^2}$ and $F = \frac{m_e \sigma}{m_i}$. The parameters $\lambda = \frac{5.65 \hbar^2 n_0^{\frac{2}{3}}}{m_e E_F}$ and $\gamma = \frac{1.6 e^2 n_0^{\frac{1}{3}}}{4\pi \varepsilon_0 E_F}$ represent the exchange and correlation respectively.

5.2.1 Derivation of Sagdeev's Potential

In order to find Sagdeev's potential, we introduce a co-moving frame defined by $\xi = l_x x + l_z z - Mt$, where $l_x, l_z = (1 - l_x^2)^{\frac{1}{2}}$ are the direction cosines and M represents the normalized phase speed of the nonlinear wave (i.e. normalized by v_A). Therefore, the set of Eqs.(5.12)-(5.15) in ξ frame can be written as:

$$v_{ez} = \frac{M}{l_z} (1 - n^{-1}), \quad (5.16)$$

$$E_z = -\frac{M}{\sigma l_z} n^{-1} \partial_\xi n^{-1} - 2l_z n \partial_\xi n + \varepsilon_0^2 l_z \partial_\xi \ln n + \gamma l_z \partial_\xi n^{\frac{1}{3}} - \lambda l_z \partial_\xi n^{\frac{2}{3}}, \quad (5.17)$$

$$\partial_\xi E_x = \frac{1}{l_x F} (n^{-1} - 1), \quad (5.18)$$

$$F l_x l_z^2 \partial_\xi E_x - F l_x^2 l_z \partial_\xi E_z = -M^2 \partial_\xi n, \quad (5.19)$$

Simplifying Eqs.(5.16-5.19), we obtain

$$\begin{aligned} & \partial_\xi^2 (\varepsilon_0^2 \ln n + \gamma n^{\frac{1}{3}} - \lambda n^{\frac{2}{3}} - \frac{M^2}{2\sigma l_z^2 n^2} - n^2 + \frac{M^2}{2\sigma l_z^2} + 1 - \gamma + \lambda) \\ &= \frac{(n^{-1} - 1)}{F l_x^2} + \frac{M^2 (n - 1)}{F l_x^2 l_z^2}. \end{aligned} \quad (5.20)$$

Now multiply Eq.(5.20) with $\partial_\xi (\varepsilon_0^2 \ln n + \gamma n^{\frac{1}{3}} - \lambda n^{\frac{2}{3}} - \frac{M^2}{2\sigma l_z^2 n^2} - n^2 + \frac{M^2}{2\sigma l_z^2} + 1 - \gamma + \lambda)$

and after some algebra (with boundary condition that at $\xi \rightarrow \pm\infty$, $n \rightarrow 1$), we obtain the following quadrature:

$$\frac{1}{2} (\partial_\xi n)^2 + K(n) = 0, \quad (5.21)$$

where $K(n)$ is the Sagdeev's potential given as:

$$K(n) = a_1 \left[\frac{b_1 + a_2 b_2 - a_3 b_3}{b_4^2} \right], \quad (5.22)$$

here $a_1 = -\frac{9n^6}{l_z^2 F}$, $a_2 = \frac{M^2}{l_z^2}$, $a_3 = \frac{1}{60l_z^4 \sigma}$, $b_1 = \frac{M^2(3n-2)}{6l_z^2 \sigma n^3} - \frac{\epsilon_0^2(1+n \ln n)}{n} - \frac{\gamma(1+2n)}{2n^{\frac{3}{2}}} + \frac{\lambda(n+2)}{n^{\frac{3}{2}}} + n(n-2)$, $b_2 = \frac{M^2(1-2n)}{2l_z^2 \sigma n^2} - \frac{n^2(2n-3)}{3} + \epsilon_0^2(n - \ln n) + \frac{\gamma(n-4)n^{\frac{1}{2}}}{4} - \frac{\lambda(2n-5)n^{\frac{3}{2}}}{5}$, $b_3 = -30M^4 - 30l_z^4 \sigma (2 + 3\gamma + 2\epsilon_0^2 - 6\lambda) + l_z^2 M^2 (10 + \sigma(20 - 45\gamma + 60\epsilon_0^2 + 36\lambda))$, $b_4 = \frac{3M^2}{l_z^2 \sigma} + 3\epsilon_0^2 n^2 + \gamma n^{\frac{7}{3}} - 2\lambda n^{\frac{8}{3}} - 6n^4$.

5.2.2 Derivation of KdV Equation

In order to see the effects of exchange-correlation and spin magnetization on the small but finite amplitude IA soliton structure, we derive the KdV equation by using standard reductive perturbation technique. Now, we use the stretched variables as follow:

$$\eta = \epsilon^{\frac{1}{2}} (z - v_0 t), \quad \zeta = \epsilon^{\frac{1}{2}} x, \quad \tau = \epsilon^{\frac{3}{2}} t, \quad (5.23)$$

where parameter $\epsilon \ll 1$ represents the amplitude of the perturbation and v_0 represents the normalized phase velocity of the wave (i.e. normalized by v_A) and the perturbed quantities can be expanded around equilibrium as follow:

$$n = 1 + \epsilon n^{(1)} + \epsilon^2 n^{(2)} + \dots, \quad (5.24)$$

$$v_{ez} = \epsilon v_{ez}^{(1)} + \epsilon^2 v_{ez}^{(2)} + \dots, \quad (5.25)$$

$$E_x = \epsilon^{\frac{1}{2}} E_x^{(1)} + \epsilon^{\frac{3}{2}} E_x^{(2)} + \dots, \quad (5.26)$$

$$E_z = \epsilon^{\frac{1}{2}} E_z^{(1)} + \epsilon^{\frac{3}{2}} E_z^{(2)} + \dots, \quad (5.27)$$

$$B_y = \epsilon^{\frac{1}{2}} B_y^{(1)} + \epsilon^{\frac{3}{2}} B_y^{(2)} + \dots, \quad (5.28)$$

Substituting Eqs.(5.23) to (5.28) into Eqs.(5.12) to (5.15) and collecting the terms of lowest order of ϵ , we obtained:

$$v_{ez}^{(1)} = v_0 n^{(1)}, \quad (5.29)$$

$$E_z^{(1)} = 0, \quad (5.30)$$

$$\partial_\zeta E_x^{(1)} = -\frac{n^{(1)}}{F}, \quad (5.31)$$

$$B_y^{(1)} = \frac{F}{v_0} E_x^{(1)}, \quad (5.32)$$

$$\partial_\zeta B_y^{(1)} = -v_0 \partial_\eta n^{(1)}, \quad (5.33)$$

Noting that the normalized phase speed v_0 at the lowest order will be simply equal to unity while in the dimensional form it is equal to v_A i.e. $v_0 = v_A$ because of loosely defined stretched variables where space and time are defined at different order. The phase speed obtained in Eq.(5.11), using the plane Fourier space by incorporating all the space and time-dependent parameters at the same linear order, depends on all quantum corrections such as Fermi pressure, spin magnetization and exchange-correlation along with Alfvén velocity and electron inertial length.

To next orders, we have:

$$-v_0 \partial_\eta n^{(2)} + \partial_\eta v_{ez}^{(2)} = -\partial_\tau n^{(1)} - \partial_\eta (n^{(1)} v_{ez}^{(1)}) \quad (5.34)$$

$$E_z^{(2)} = \left[-\frac{v_0^2}{\sigma} - 2\partial_\eta n^{(1)} + \varepsilon_0^2 \partial_\eta n^{(1)} + \frac{\gamma}{3} \partial_\eta n^{(1)} - \frac{2\lambda}{3} \partial_\eta n^{(1)} \right] \quad (5.35)$$

$$-v_0 \partial_\eta n^{(2)} - F v_0 \partial_\zeta \partial_\eta E_x^{(2)} = -\partial_\tau n^{(1)} - F \partial_\zeta \partial_\tau E_x^{(1)} + F v_0 \partial_\zeta \partial_\eta E_x^{(1)} \quad (5.36)$$

$$\partial_\eta B_y^{(2)} = \frac{F}{v_0} \partial_\eta E_x^{(2)} - \frac{F}{v_0} \partial_\zeta E_x^{(2)} + \frac{1}{v_0} \partial_\tau B_y^{(1)} \quad (5.37)$$

$$\partial_\zeta \partial_\eta B_y^{(2)} = -v_0 \partial_\eta n^{(2)} + \partial_\tau n^{(1)} \quad (5.38)$$

We first eliminate $B_y^{(2)}$ from Eq.(5.38) and $E_x^{(2)}$ from Eq.(5.37). Then subtracting Eq.(5.34) from the resulting equation we finally get the desired equation:

$$\partial_\tau n^{(1)} - \frac{v_0}{2} n^{(1)} \partial_\eta n^{(1)} + \frac{v_0}{2} \partial_\zeta n^{(1)} \partial_\eta E^{(1)} + \frac{v_0}{2} F \Lambda \partial_\zeta^2 \partial_\eta n^{(1)} = 0. \quad (5.39)$$

where $\Lambda = (\varepsilon_0^2 + \frac{\gamma}{3} - \frac{2\lambda}{3} - \frac{v_0^2}{\sigma} - 2)$. Eqs.(5.31) and (5.39) give the evolution of the solitary IAWs. Moreover, using planar coordinate $\mu = l_x \zeta + l_z \eta - \Delta \tau$ the stationary travelling wave solution of Eq.(5.39) is given by

$$\bar{n} = -A \sec h^2[W\mu], \quad (5.40)$$

where A and W are the amplitude (i.e. maximum potential perturbation) and the width (i.e. spatial extension) of the localized pulse such that $A = 3 \left(\frac{\Delta}{v_0 l_z} \right)$ and $W = \sqrt{\frac{\Delta}{F \Lambda l_x l_z}}$ with $\Delta = M - 1$. By ignoring the quantum effects(e.g. Fermi pressure, exchange-correlation and spin magnetization), the soliton solution of Ref.[1] can be retrieved for classical plasmas.

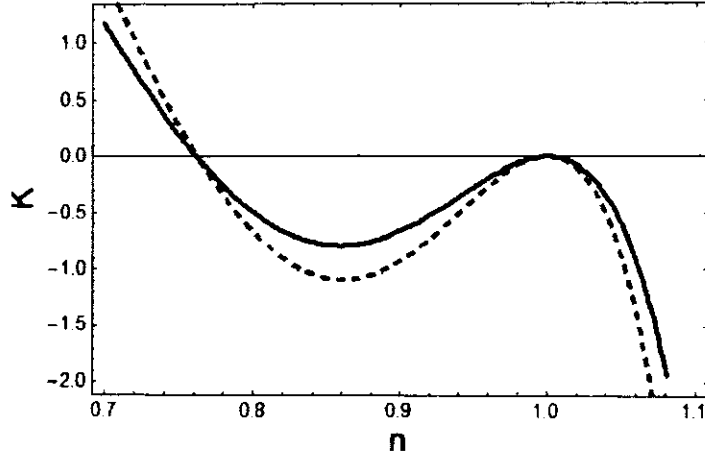


Figure 5.1: Sagdeev's potential $K(n)$ is plotted against number density n from Eq.(5.22) for different values of number density (i.e. exchange-correlation), such that (i) $n_0 \approx 1.7 \times 10^{32} m^{-3}$ (Bold) with $g_Q = 0.9$, $T_{Fe} \approx 1.3 \times 10^7 (^{\circ}K)$, $\gamma \approx 0.11$, $\lambda \approx 1.18$, $\alpha \approx 0.0006$. (ii) $n_0 \approx 1 \times 10^{33} m^{-3}$ (Dashed) with $g_Q = 0.0.5$, $T_{Fe} \approx 4.20 \times 10^7 (^{\circ}K)$, $\gamma \approx 0.06$, $\lambda \approx 1.18$, $\alpha \approx 0.13$. Other parameters are $B_0 = 10^8$, $M = 1.1$, $l_x = 0.3$.

5.3 Numerical Analysis and Discussion

Dense plasmas existing in astrophysical compact stars such as white dwarfs, pulsars, and magnetars are characterized by strong magnetic fields $B \approx 10^7 - 10^{11} T$, whereas the plasma number densities are thought to have $n_0 \approx 10^{29} - 10^{33} m^{-3}$ [, ,]. Usually, we use quantum coupling parameter g_Q to describe the collisional or collisionless state of quantum plasma. The coupling parameter is given as $g_Q = \varepsilon_{int}/\varepsilon_{Fe}$, where $\varepsilon_{int} = e^2/4\pi\epsilon_0 (3/4\pi n_0)^{1/3}$ is the interaction energy with ϵ_0 being the dielectric permeability in vacuum and $\varepsilon_{Fe} = \frac{\hbar^2}{2m} (3n_0\pi^2)^{2/3}$ is the Fermi energy. It is to be noted from the expression of the quantum coupling parameter that at higher values of plasma densities, the collective effects dominate in quantum plasma. In the mks system, the lowest plasma density becomes $n_0 \geq 1.24 \times 10^{32} m^{-3}$ for $g_Q = 1$. Numerically, we have exchange-correlation in the form $\lambda \approx 3.84 \times 10^{-22} n_0^{2/3}$ and $\gamma \approx 2.07 \times 10^{-12} n_0^{1/3}$. Whereas, the magnetization energy can be written as $\varepsilon_0 \approx 2.2 \times 10^{-9} (B_0/n_0^{2/3})$. It can easily be observed that the exchange-correlation depends only on number density whereas normalized Zeeman energy ε_0 depends on both magnetic field strength and plasma number density. Now we present the numerical analysis of Eqs.(5.22) and(5.40) by changing the values of number density and magnetic field strength in Figures (5.1-5.3).

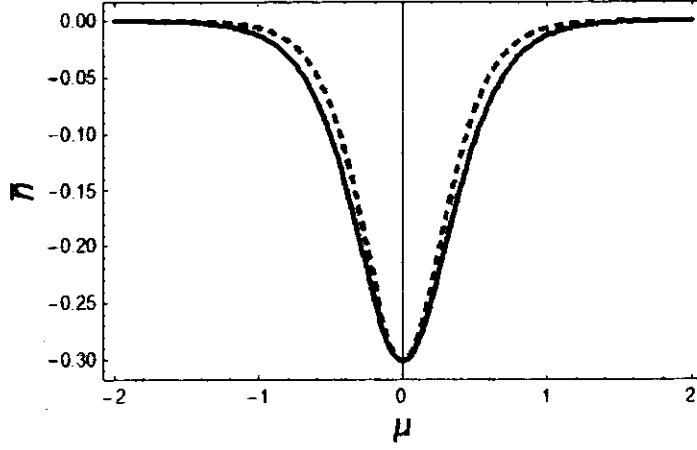


Figure 5.2: The corresponding dip soliton is plotted between \bar{n} and μ of Figure 5.1 using Eq.(5.40) for different value of number density (i.e. exchange-correlation). All parameters are same as in Figure 5.1.

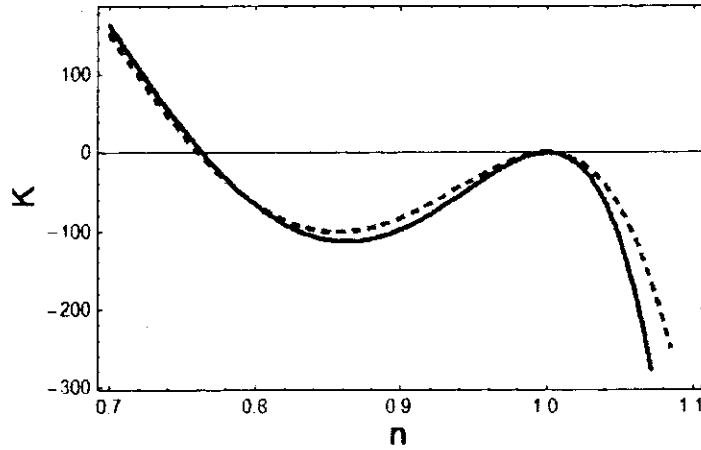


Figure 5.3: Profile of Sagdeev's potential curves $K(n)$ against number density n using Eq.(5.22) for different values of magnetic field strength (spin magnetization energy), such that (i) $B_0 = 3 \times 10^7 T$ (Bold) with $\varepsilon_0 \approx 1.5$ and $\alpha \approx 0.07$. (ii) $B_0 = 1 \times 10^8 T$ (Dashed) with $\varepsilon_0 \approx 5.2$ and $\alpha \approx 0.007$. Other parameters are $M = 1.1$, $l_x = 0.3$, $n_0 \approx 1.7 \times 10^{32} m^{-3}$, $T_F \approx 1.3 \times 10^7 (^{\circ}K)$ and $g_Q = 0.9$.

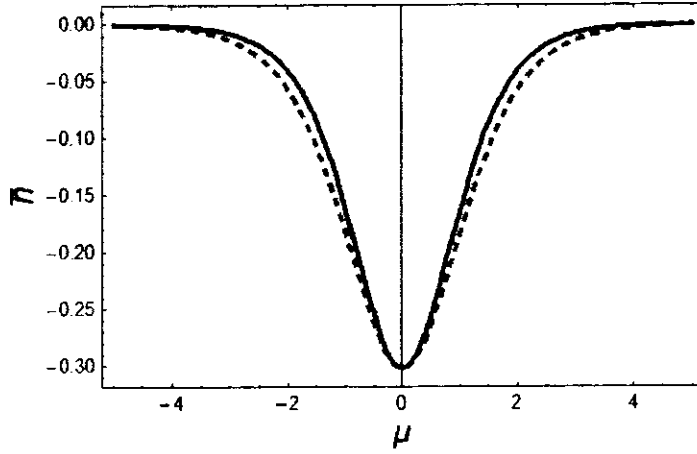


Figure 5.4: The corresponding dip soliton is plotted between \bar{n} and μ of Figure 5.3 using Eq.(5.40) for different values of magnetic field strength (spin magnetization energy). All parameters are same as in Figure 5.3.

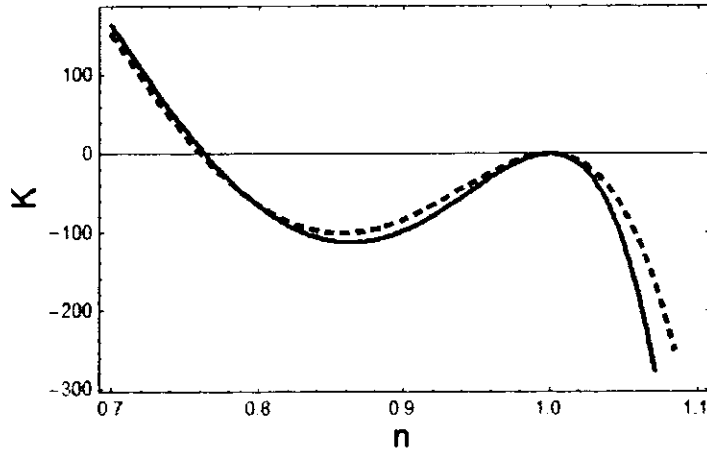


Figure 5.5: Sagdeev's potential $K(n)$ using Eq.(5.22) for different values of magnetic field strength (ε_0) with fixed value of $\gamma \approx 0.11$ and $\lambda \approx 1.18$. All parameters are same as in Figure 5.3.

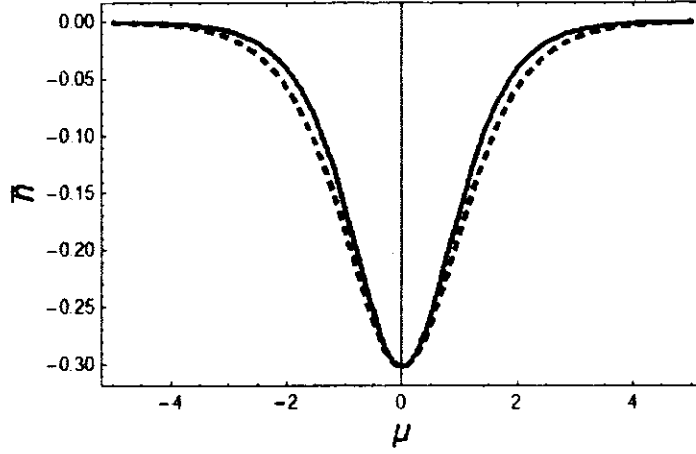


Figure 5.6: The corresponding dip soliton using Eq.(5.40) for different values of magnetic field strength (ε_0). All parameters are same as in Figure 5.5.

The effects of exchange-correlation on IAWs by changing the values of number density (i.e. λ and γ) while ignoring the value of spin magnetization effects altogether (i.e. $\varepsilon_0 = 0$) are shown in Figures (5.1-5.2). The profiles of Sagdeev's potential for different values of number density are shown in Figure 5.1. It can be observed from Figure 5.1 that the Sagdeev potential curve gives dip soliton for $M > 1$ in super-Alfvénic region under condition $n_m < n < 1$. Also, by increasing the value of parameters λ and γ (i.e. number density), the depth of Sagdeev potential curves are increasing while the crossing point n_m (i.e. amplitude) will remain the same in Figure 5.1. The corresponding dip soliton structure of Figure 5.1 is shown in Figure 5.2. It is evident from Figure 5.2 that the width of dip soliton is narrowing by enhancing the value of parameters λ and γ while no change observed in amplitude. This kind of dip soliton in the super-Alfvénic region is reported in most of the literature [14, 15].

The effects of spin magnetization on IAWs by changing the values of the magnetic field (i.e. ε_0) while ignoring exchange-correlation effects are shown in Figures (5.3-5.4). The Sagdeev potential curves for different value of magnetic field (i.e. ε_0) are shown in Figure 5.3. It is to be noted from Figure 5.3 that the Sagdeev potential curve under condition $n_m < n < 1$ can forms dip soliton in the super-Alfvénic region for $M > 1$. It is further found that by increasing the value of magnetic field strength (i.e. spin magnetization), the depth of Sagdeev potential curves are decreasing while the crossing

point n_m (i.e. amplitude) will remain the same. The corresponding soliton structure of Figure 5.3 is shown in Figure 5.4. It is clear from Figure 5.4 that the width of soliton is increasing by enhancing the value of magnetic field strength (i.e. ε_0) while, no change observed in soliton amplitude.

In the presence of both exchange-correlation (i.e. λ and γ) and spin magnetization (i.e. ε_0) effects, we have found again dip soliton with $M > 1$ being in the super-Alfvénic region as shown in Figures (5.5-5.6). The Sagdeev potential curves for different values of magnetic field strength (i.e. ε_0) while keeping the value of number density fixed (i.e. $\lambda = \gamma = \text{const}$) are shown in Figure 5.5. It is observed from Figure 5.5 that the depth of Sagdeev potential profiles are decreasing with the increasing value of magnetic field strength (i.e. ε_0) whereas no change is found in crossing point n_m (i.e. amplitude). The corresponding inertial Alfvén dip soliton of Figure 5.5 is shown in Figure 5.6. It is revealed from Figure 5.6 that the width of inertial Alfvén dip soliton is enhancing by increasing the value of parameter ε_0 while no change observed in amplitude.

Noting that for both exchange-correlation (i.e. λ and γ) and spin magnetization (i.e. ε_0) effects, the super inertial Alfvénic solitons with density dip have a strong dependency on spin magnetization rather than on density correlation. Also, in the presence of quantum effects, the system support only super inertial Alfvénic solitons having density dip structures. Moreover, due to the incorporation of spin effects the total magnetic pressure is enhancing as compared to Fermi pressure which makes β very low and hence increasing the inertial effects of electrons for the studying IAWs in magnetized quantum plasma.

5.4 Summary

We have investigated the nonlinear propagation characteristics of inertial Alfvén waves in low- β quantum plasmas by taking into account spin magnetization and exchange-correlation effects for the case $\alpha \equiv \beta/2Q \ll 1$. The Sagdeev potential was derived by using two potential approximation, whereas KdV equation was derived by employing the reductive perturbation technique. Both approaches provided the numerical results

which are inconsistent with each other. In the presence of spin magnetization and exchange-correlation effects, we have found only inertial Alfvénic solitons having density dip structures. Furthermore, inertial Alfvén dip soliton moves with super-Alfvénic wave speed. The numerical values of plasma density and magnetic field strength were used in accordance to astrophysical dense plasma situations that can exist in compact stars. Our results are valid for astrophysical compact objects like, white dwarfs, magnetars, and pulsars, where strong magnetic field and high number density plasmas exist.

Bibliography

- [1] U. Inan and M. Golkowski, *Principles of Plasma Physics for Engineers and Scientists* (Cambridge University Press, 2011).
- [2] F. F. Chen, *Introduction to Plasma physics and controlled Fusion* (Plenum Press, New York, 1984).
- [3] G. Manfredi, *Fields Inst. Commun.* **46**, 263(2005).
- [4] G. Manfredi and J. Hurst, *Plasma Phys. Control. Fusion* **57**, 054004 (2015).
- [5] D. Koester and G. Chanmugam, *Rep. Prog. Phys.* **53**, 837 (1990).
- [6] G. Chabrier, F. Douchin and A. Y. Potekhin, *J. Phys: Condens. Matter* **14**, 9133 (2002).
- [7] G. Chabrier, D. Saumon and A. Y. Potekhin, *J. Phys. A: Math. Gen.* **39**, 4411 (2006).
- [8] F. Haas, *Quantum Plasmas: An Hydrodynamic Approach* (Springer, New York, 2011).
- [9] B. Eliasson and P. K. Shukla, *Phys. Scr.* **78**, 025503 (2008).
- [10] F. Haas and S. Mahmood, *Phys. Rev. E* **92**, 053112 (2015).
- [11] L. Lewin, *Polylogarithms and Associated Functions* (North Holland, NewYork,1981)
- [12] A. E. Dubinov and I. N. Kitaev, *Phys. Plasmas* **21**, 102105 (2014).

- [13] P. M. Bellan, *Fundamentals of Plasma Physics* (Cambridge University Press, 2006).
- [14] N. F. Cramer, *The Physics of Alfvén Waves* (John Wiley & Sons, 2001).
- [15] H. Washimi and T. Taniuti, *Phys. Rev. Lett.* **17**, 996 (1966).
- [16] R. Z. Sagdeev, *Reviews of Plasma Physics*, New York Consultant Bureau, **4**, 52, (1966).
- [17] D. J. Korteweg and H. de Vries, On the change of form of long waves advancing in a rectangular canal, and on a new type of long stationary waves. *Philosophical Magazine*, **39**, 422 (1895)
- [18] R. C. Davidson, *Methods in Nonlinear Plasma Theory* (Academic Press, 1972).
- [19] P. Ludwig, K. Balzer, A. Filinov, H. Stolz, and M. Bonitz, *New J. Phys.* **10**, 083031 (2008).
- [20] G. Manfredi, P.-A. Hervieux, Y. Yin, and N. Crouseilles: *Collective Electron Dynamics in Metallic and Semiconductor Nanostructures*. *Lect. Notes Phys.* **795**, 1–44 (2010).
- [21] Markowich, P. A., Ringhofer, C. A., Schmeiser, C.: *Semiconductor equations*, Springer, Vienna, (1990).
- [22] T. C. Killian, *Science* **316**, 705 (2007).
- [23] S. H. Glenzer, O. L. Landen, P. Neumayer, R. W. Lee, K. Widmann, S. W. Pollaine, R. J. Wallace, G. Gregori, A. Holl, T. Bornath, R. Thiele, V. Schwarz, W.-D. Kraeft, and R. Redmer, *Phys. Rev. Lett.* **98**, 065002 (2007).
- [24] A. K. Harding and D. Lai, *Rep. Prog. Phys.* **69**, 2631 (2006).
- [25] L. Stenflo, P. K. Shukla, and M. Marklund, *Europhys. Lett.* **74**, 844 (2006) .
- [26] W. F. El-Taibany and M. Waidati, *Phys. Plasmas* **14**, 042302 (2007).

- [27] S. Ali, W. M. Moslem, P. K. Shukla, and R. Schlickeiser, *Phys. Plasmas* **14**, 082307 (2007).
- [28] P. K. Shukla and L. Stenflo, *Phys. Lett. A* **355**, 378 (2006).
- [29] S. Chandrasekhar, *Mon. Not. R. Astron. Soc.* **95**, 207 (1935).
- [30] D. Melrose, *Quantum Plasmadynamics - Unmagnetized Plasmas* (Springer-Verlag, New York, 2008).
- [31] D. B. Melrose and A. Mushtaq, *Phys. Rev. E* **82**, 056402 (2010).
- [32] D. B. Melrose and A. Mushtaq, *Phys. Plasmas* **17**, 122103 (2010).
- [33] F. Haas and S. Mahmood, *Phys. Rev. E* **94**, 033212 (2016).
- [34] F. Haas, *Phys. Plasmas* **12**, 062117 (2005).
- [35] G. Manfredi and F. Haas, *Phys. Rev. B* **64**, 075316 (2001).
- [36] C. Gardner, *SIAM J. Appl. Math.* **54**, 409 (1994).
- [37] F. Haas, G. Manfredi, and M. R. Feix, *Phys. Rev. E* **62**, 2763 (2000).
- [38] F. Haas, L. G. Garcia, J. Goedert, and G. Manfredi, *Phys. Plasmas* **10**, 3858 (2003).
- [39] D. Shaikh and P. K. Shukla, *Phys. Rev. Lett.* **99**, 125002 (2007).
- [40] P. K. Shukla and B. Eliasson, *Phys. Rev. Lett.* **99**, 096401 (2007).
- [41] P. K. Shukla, *Nat. Phys.* **5**, 92 (2009).
- [42] M. Marklund and G. Brodin, *Phys. Rev. Lett.* **98**, 025001 (2007).
- [43] L. Wei and Y. N. Wang, *Phys. Rev. B* **75**, 193407 (2007).
- [44] N. Crouseilles, P.-A. Herveix, and G. Manfredi, *Phys. Rev. B* **78**, 155412 (2008).
- [45] G. Brodin and M. Marklund, *New J. Phys.* **9**, 277 (2007).

- [46] P. K. Shukla and B. Eliasson, *Phys. Usp.* **53**, 51 (2010).
- [47] G. Brodin and M. Marklund, *Phys. Plasmas* **14**, 112107 (2007).
- [48] M. Marklund, B. Eliasson, and P. K. Shukla, *Phys. Rev. E* **76**, 067401 (2007).
- [49] J. W. Belcher and L. Davis, *J. Geophys. Res.* **76**, 3534 (1971).
- [50] R. Z. Sagdeev, and A. A. Galeev, *Nonlinear Plasma Theory* (W. A. Benjamin, New York, 1969).
- [51] P. Louarn, J. E. Wahlund, T. Chust, H. de Feraudy, A. Roux, B. Holback, P. O. Dovner, A. I. Eriksson, and G. Holmgren, *Geophys. Res. Lett.* **21**, 1847 (1994).
- [52] P. O. Dovner, A. I. Eriksson, R. Boström, and B. Holback, *Geophys. Res. Lett.* **21**, 1827 (1994).
- [53] A. Hasegawa and K. Mima, *Phys. Rev. Lett.* **37**, 690 (1976).
- [54] C. K. Goertz, and R. Boswell, *J. Geophys. Res.* **84**, 7239(1979).
- [55] R. L. Lysak and C. T. Dum, *J. Geophys. Res.* **88**, 365 (1983).
- [56] M. Y. Yu and P. K. Shukla, *Phys. Fluids* **21**, 1457 (1978).
- [57] P. K. Shukla, H. D. Rahman, and R. P. Sharma, *J. Plasma Phys.* **28**, 125 (1982).
- [58] M. K. Kalita and B. C. Kalita, *J. Plasma Phys.* **35**, 267 (1986).
- [59] R. K. Roychoudhury, and P. Chatterjee, *Phys. Plasmas* **5**, 3828 (1998).
- [60] Y. Chen, Z. Y. Li, and W. Liu, and Z.-D. Shi, *Phys. Plasmas* **7**, 371 (2000).
- [61] D. J. Wu and J. K. Chao, *Nonlin. Processes Geophys.* **11**, 631 (2004).
- [62] N. Devi, R. Gogoi, G. C. Das, and R. Roychoudhury, *Phys. Plasmas* **14**, 012107 (2007).
- [63] H. Saleem and S. Mahmood, *Phys. Plasmas* **10**, 2612 (2003).
- [64] S. Mahmood, and H. Saleem, *Phys. Plasmas* **10**, 4680 (2003).

- [65] A. M. Mahmood, S. Mahmood, A. M. Mirza, H. Saleem, *Chin. Phys. Lett.* **22**, 632(2005).
- [66] S. A. Khan, *Astrophys. Space Sci.* **343**, 683 (2013).
- [67] B. B. Kadomtsev, *The Plasma Turbulence* (Academic, New York, 1965).
- [68] A. Hasegawa and C. Uberoi, *The Alfvén Wave*, DOE Critical Review Series-Advances in Fusion Science and Engineering (Technical Information Center, U.S. Department of Energy, Washington, DC, 1982).
- [69] S. A. Khan and H. Saleem, *Phys. Plasmas* **16**, 052109 (2009).
- [70] J. E. Wahlund, P. Louarn, T. Chust, H. de Feraudy, A. Roux, B. Holback, P.-O. Dovner, and G. Holmgren, *Geophys. Res. Lett.*, **21**, 1831-1834, (1994).
- [71] C. C. Chaston, L. M. Peticolas, C. W. Carlson, J. P. McFadden, F. Mozer, M. Wilber, G. K. Parks, A. Hull, R. E. Ergun, R. J. Strangeway, M. Andre, Y. Khotyaintsev, M. L. Goldstein, M. Acuña, E. J. Lund, H. Reme, I. Dandouras, A. N. Fazakerley, and A. Balogh, *J. Geophys. Res.* **110**, 10483 (2005).
- [72] B. Buti and P. KShukla.:*Phys. Lett. A* **74**, 409 (1979).
- [73] G. Brodin, M. Marklund, L. Stenflo, and P. K. Shukla, *New J. Phys.* **8**, 16 (2006).
- [74] M. Marklund, G. Brodin, :*Phys. Rev. Lett.* **98**, 25001 (2007).
- [75] M. Marklund, B. Eliasson, and P. K. Shukla, *Phys. Rev. E* **76**, 067401(2007).
- [76] A. Mushtaq, S. V. Vladimirov.:*Phys. Plasmas* **17**, 102310 (2010).
- [77] A. Mushtaq, S. V. Vladimirov.:*Eur. Phys. J. D* **64**, 419 (2011).
- [78] A. Mushtaq, R. Maroof, Z. Ahmad, A. Qamar.:*Phys. Plasmas* **19**, 052101 (2012).
- [79] R. Maroof,S. Ali, A. Mushtaq, A.Qamar, *Plasmas* **22**, 112102 (2015).
- [80] L. Landau.:*Z. Phys.* **64**, 629 (1930).

- [81] R. K. Pathria.:*Statistical Mechanics* p. 202, Butterworth-Heinemann, Oxford,(1996)
- [82] Qiang-Lin Hu, Shen-Lin Zhou, Xiao-Guang Yu, Gui-Lan Xiao, Xiao-Bing Luo, and Ren-Ping Cao *Phys. Plasmas* **23**, 112113 (2016).
- [83] V. S. Beskin, , A. V. Gurevich, N. Ya. :Istomin, *Physics of the Pulsar Magnetosphere* Cambridge University Press, Cambridge, (1993).
- [84] C. Kouveliotou, D. Dieters, T. Strohmayer, J.van Paradijs, G. J. Fishman, C. A. Meegan, K. Hurley, J. Kommers, I. Smith, D. Frail.:*Nature London* **393**, 235 (1998).
- [85] T. Padmanabhan, :*Theoretical Astrophysics: Stars, Stellar Systems*, Vol. II (Cambridge University Press, London, 2001).
- [86] S. L. Shapiro and S. A. Teukolsky, *Black Holes, White Dwarfs, and Neutron Stars: The Physics of Compact Objects* (Wiley, New York, 1983).
- [87] P. Zoller et al., *Eur. Phys. J. D* **36**, 203 (2005).
- [88] P. K. Shukla, B. Eliasson, *Rev. Mod. Phys.* **83**, 885(2011) .
- [89] L. Brey, J. Dempsey, N.F. Johnson, B.I. Halperin, *Phys. Rev. B* **42**,1240 (1990)
- [90] S. Mao, J. Xue, *Phys. Scr.* **84**, 055501(2011).
- [91] Yu-Ting Ma, Sheng-Hong Mao, and Ju-Kui Xue, *Phys. Plasmas* **18**, 102108 (2011).
- [92] K. Ourabah and M. Tribeche, *Phys. Rev. E* **88**, 45101 (2013).
- [93] H. Cai-Xia and X. Ju-Kui, *Chin. Phys. B* **22**, 025202 (2013).
- [94] K. Mebrouk and M. Tribeche, *Phys. Lett. A* **378**,3523 (2014).
- [95] R. Maroof, A. Mushtaq, and A. Qamar, *Phys. Plasmas* **23**, 013704 (2016).

- [96] T. Rimza and P. Sharmaa, IOP Conf. Series: Journal of Physics: Conf. Series **836**,012028 (2017) .
- [97] B. Sahu and A.P. Misra, Eur. Phys. J. Plus **132**, 316(2017).
- [98] G. Brodin, A. P. Misra and M. Marklund, Phys. Rev. Lett. **105** 105004(2010).
- [99] P.A. Andreev, Phys. Rev. E **91**, 033111 (2015).
- [100] P.A. Andreev and L.S. Kuz'menkov, Annals of Physics **361**, 278–292 (2015).
- [101] N. Sadiq and A. Mushtaq Ahmad, Plasma Res. Express **1**, 025007 (2019).
- [102] R. J. Stefant, Phys. Fluids **13**, 440 (1970).
- [103] P. K.Shukla, L. Stenflo, and R. Bingham ,Phys. Plasmas **6**, 1677 (1999).
- [104] F. Schwabl, *Statistical Mechanics* (Springer-Verlag Berlin Heidelberg 2006).
- [105] P. Hohenberg and W. Kohn, Phys. Rev. **136**, B864 (1964).
- [106] W. Kohn and L. J. Sham, Phys. Rev. **140**, A1133 (1965).
- [107] N. Sadiq, and A. Mushtaq, Phys. Plasmas **25**, 124501 (2018).